

Analytical and numerical analysis of spillover effects in prioritized PrEP for HIV prevention

Chiara Piazzola^a, Salman Safdar^b, Alex Viguerie^{c,*} and Abba B. Gumel^{d,e,f}

^a Department of Mathematics, Technical University of Munich, 85748 Garching bei München, Germany

^b Department of Mathematics, University of Karachi, University Road 75270, Pakistan

^c Department of Pure and Applied Sciences, Università degli Studi di Urbino Carlo Bo, Urbino, PU 60129, Italy

^d Department of Mathematics, University of Maryland, College Park, MD, 20742, USA

^e Institute for Health Computing, University of Maryland, North Bethesda, Maryland, 20852, USA

^f Department of Mathematics and Applied Mathematics, University of Pretoria, Pretoria 0002, South Africa

ABSTRACT

Pre-exposure prophylaxis (PrEP) is a highly effective intervention for preventing HIV transmission, but its high cost and uneven uptake raise key challenges for allocating resources efficiently. While *spillover effects* - wherein PrEP use in one group reduces infections in others - are known to occur, they remain poorly quantified and rarely guide policy. We develop and analyze a novel compartmental HIV model that stratifies the population into three interacting subgroups: heterosexual males (HETM), heterosexual females (HETF), and men who have sex with men (MSM). Our baseline model assumes idealized PrEP effectiveness and full compliance, enabling rigorous analytical treatment while preserving key epidemiological features. We derive standard results, including the control reproduction number, and establish conditions for local and global stability of the disease-free equilibrium.

Crucially, we provide a closed-form, time-resolved expression for the *spillover-adjusted number needed to treat* (NNT), a measure of the population-level impact of PrEP uptake in one group on incidence in others. Simulations calibrated to Georgia state-level data reveal that PrEP delivery to MSM yields substantial indirect benefits, particularly for HETF, where the spillover effect exceeds the direct effect by a factor of five. We extend the baseline model to include risk stratification within HETF, showing that targeting high-risk HETF outperforms direct PrEP delivery to HETM, emphasizing the importance of intra-group heterogeneity.

To evaluate whether these findings persist under more detailed assumptions, we embed our framework into the national *HOPE model* maintained by the CDC and conduct global sensitivity analysis using Sobol indices. This approach extends our analytical insights and quantifies how uncertainty in PrEP allocation strategies propagates through complex epidemic dynamics. Taken together, our results show that moderately complex, analytically tractable models can yield realistic, cost-effective, and actionable guidance for HIV control - capturing nonlinear spillover dynamics in ways that remain interpretable even within high-dimensional national-scale simulations.

Keywords HIV; spillover; pre-exposure prophylaxis (PrEP); sensitivity analysis.

* Corresponding author: Email: alexander.viguerie@uniurb.it

1 Introduction

Since its approval by the United States Food and Drug Administration (FDA) in 2012, pre-exposure prophylaxis (PrEP) has emerged as a critical tool in the fight against the human immunodeficiency virus (HIV), the causative agent of

acquired immune deficiency syndrome (AIDS) [1]. Despite major biomedical advances, HIV remains a pressing global health concern: as of 2023, an estimated 39 million people worldwide were living with HIV, with 1.3 million new infections occurring annually [2]. In the United States alone, approximately 1.2 million people are living with HIV, and over 30,000 new cases are reported each year, with a disproportionate burden among men who have sex with men, Black and Latino communities, and residents of the southeastern states [2]. This persistent disease burden underscores the importance of optimizing prevention strategies like PrEP.

Studies have demonstrated that optimal or consistent PrEP use (daily or at least 4 times per week) can reduce the risk of acquiring HIV infection from sexual contact by up to 99% [3, 4, 5, 6, 7, 8], and from injection drug use by up to 84% [9, 10]. In the years since its initial release under the brand name *Truvada*, an additional daily PrEP treatment (*Descovy*) as well as a long-acting injectable variant (*Apretude*) have been approved and introduced in the United States [11, 12]. Due to its high efficacy and potential in reducing HIV incidence, expanding PrEP coverage is a core component of the Ending the HIV Epidemic (EHE) initiative, which aims to reduce annual HIV incidence in the United States by 90% by 2030 [13]. Data from the United States Centers for Disease Control and Prevention (CDC) showed that, in 2021, only 30% of PrEP-eligible individuals in the United States had an active PrEP prescription [14, 15]. Although this is a substantial increase from 13.2% in 2018, it falls short of the EHE target of 50% by 2025 [16, 14, 17].

Rates of PrEP coverage vary by group. For instance, while 34.2% of PrEP-eligible males had an active PrEP prescription in 2021, this figure was only 12.4% among females¹. Significant disparities were also observed among racial/ethnic groups [14]. Expanding PrEP coverage to ensure increased, more equitable access to PrEP is an important goal of current and future HIV prevention and control efforts [18]. Additionally, PrEP eligibility guidelines have been regularly revised since their initial introduction, and expanding PrEP eligibility to additional high-risk populations may also further aid HIV prevention efforts [11, 19, 17].

While the benefits of increased PrEP use on HIV incidence are clear, unfortunately PrEP is also quite expensive. Specifically, brand name versions of the drug may cost as much as \$22,000 for an annual treatment regimen for one patient [20]. Modeling analyses have shown that, under certain circumstances, targeted administration of PrEP may not be cost-effective [21, 22, 23]. Ensuring that PrEP is allocated in a manner such that its benefits in HIV incidence reduction are maximized, while minimizing additional costs as much as possible, is therefore a subject of interest in HIV prevention efforts in the United States and globally.

Recent modeling analyses of PrEP have shown that PrEP uptake often results in *spillover effects*, wherein increased PrEP use in one group results in the reduction of HIV incidence in a separate group, and that such effects may be substantial [24, 21, 22]. Thus, owing to this (spillover) phenomenon, greater reduction in HIV incidence in one group may be achieved by increasing PrEP coverage in another. HIV intervention and control efforts that leverage the spillover effects, therefore, offer significant potential in reducing HIV incidence at lower cost.

Several modeling studies have shown evidence of PrEP spillover effect (through numerical simulations). to the authors' knowledge, no modeling study has addressed this issue specifically and rigorously. In some cases, the authors explicitly noted and discussed these effects [21]; in other instances, spillover effects were apparent from the provided results, however, the authors did not discuss them specifically [24]. To the authors' knowledge, however, no modeling study has attempted to address this issue specifically and rigorously. A possible reason why this question has not received further attention is that the direct study of spillover effects is not straightforward.

At a basic level, PrEP spillover results from the interaction between distinct populations or *population mixing*. Analysis of population mixing in infectious disease models more generally has received attention over the years (see, for instance, [25, 26, 27, 28, 29, 30, 31, 32]). However, the most commonly-employed techniques in these analyses generally rely on a linearization of the mathematical model about an equilibrium at a specific point in time. These approaches are ill-suited to study PrEP spillover effects, which are nonlinear and time-dependent in nature. In particular, a relatively long time duration (many years) may be necessary for the real effect of spillover to be noticeable at population-level [21]. Furthermore, the contact patterns relevant for HIV transmission are quite distinct from the more well-understood preferential mixing models, which are more amenable to standard linearization analysis techniques [25, 29, 28].

The objective of the current study is to develop a novel mathematical modeling framework for realistically quantifying the impact of PrEP spillover effects on the control of HIV spread in a population. Specifically, we construct a simplified compartmental model that stratifies the total population into three subgroups: heterosexual males (HETM), heterosexual females (HETF), and men who have sex with men (MSM). This basic model, which is calibrated using HIV data from the U.S. state of Georgia, is rigorously analyzed to investigate the asymptotic stability of the disease-free equilibrium, characterize spillover effects, and derive closed-form expressions for the *number needed to treat* (NNT) in each subgroup—a commonly used metric to quantify PrEP effectiveness in populations [33, 34, 35, 19].

¹The terms 'male' and 'female' in this article refer to sex defined at birth.

These analyses enable us to assess how varying levels of PrEP coverage in each subgroup affect HIV incidence within and across groups over time. The model is then extended to include risk stratification within the HETF population, dividing it into low- and high-risk subpopulations. The paper is organized as follows. The basic model is formulated in Section 2, where detailed analyses of spillover dynamics and NNT are presented. Section 3 extends the model to include HETF risk heterogeneity. In Section 4, we apply the modeling and analytical insights developed from the simplified models to the HOPE model—a large-scale compartmental model of HIV transmission developed by the CDC [36, 23, 37, 38]. Since standard analytical methods are not easily applicable to a model of this size and complexity, we employ a polynomial chaos expansion (PCE)-based Sobol sensitivity analysis [39, 40] to study spillover effects, demonstrating that Sobol indices can effectively quantify intergroup spillover in time. Finally, in Section 5 we summarize our findings, contextualize them within the broader HIV modeling literature, and provide conclusions and directions for future work.

2 Basic model for sexual HIV transmission

Mathematical modeling of HIV transmission is complex, due to significant post-infection factors, including testing/diagnosis, treatment adherence, and differential infectivity, which must be considered in general [37, 24, 36, 21]. However, in the current study, we focus on the independent effects of PrEP, which acts on the *susceptible* population, and is of no further use post-infection. This allows us to consider a simplified structure consisting of a susceptible compartment S and a single infected compartment I , which represents the average of the entire population of persons with HIV (PWH) in terms of awareness, disease stage, and treatment status. Note that, for simplicity, we assume PrEP is perfectly efficacious (i.e., a PrEP user has no chance of acquiring HIV), and further, that the PrEP users are perfectly adherent. For simplicity, we focus on sexual transmission HIV, which accounts for 93% of new infections in the U.S. [2].

We assume that the total population at time t is subdivided into three subgroups: *Men who have sex with men* (MSM, denoted with subscript msm), *Heterosexual females* (HETF, denoted with subscript $hetf$), and *Heterosexual males* (HETM, denoted with subscript $hetm$). The total populations of each subgroup are denoted as $N_{msm}(t)$, $N_{hetf}(t)$, and $N_{hetm}(t)$, respectively. Furthermore, we divide each subgroup into mutually exclusive subpopulations of susceptible S and infected I populations. Hence, the total number of individuals in each of the subgroups at time t , is given by:

$$N_{msm}(t) = S_{msm}(t) + I_{msm}(t), \quad N_{hetm}(t) = S_{hetm}(t) + I_{hetm}(t), \quad N_{hetf}(t) = S_{hetf}(t) + I_{hetf}(t),$$

with the total population (in all subgroups) at time t , denoted by $N(t)$, given by:

$$N(t) = N_{msm}(t) + N_{hetf}(t) + N_{hetm}(t).$$

The three transmission groups interact following the contact structure depicted in Fig. 2.1. Briefly, HETM interact only with HETF, HETF interact with both MSM and HETM, and MSM interact with HETF as well as among themselves. The probabilities of HIV transmission per male to male contact, per female to male contact, and per male to female contact, are denoted by β_M^M , β_M^F , and β_F^M , respectively. Additionally, the susceptible population is increased by the recruitment of individuals into the sexually active population at a rate Π_j with $j = \{msm, hetf, hetm\}$. HIV-infected individuals in each subgroup j die due to the disease at a rate δ_j , while natural death occurs in all sub-populations at a rate μ . Finally, it is assumed that PrEP is administered to a fraction of sexually active susceptible individuals ε_j in each subgroup j . Hence, the basic model for sexual transmission of HIV is given by the following system of nonlinear differential equations:

$$\left\{ \begin{array}{l} \frac{dS_{msm}}{dt} = \Pi_{msm} - a_{msm}(1 - \varepsilon_{msm}) \left[\eta_{msm} \beta_M^M \frac{I_{msm}}{N_{msm}} + (1 - \eta_{msm}) \beta_F^M \frac{I_{hetf}}{N_{hetf}} \right] S_{msm} - \mu S_{msm}, \\ \frac{dI_{msm}}{dt} = a_{msm}(1 - \varepsilon_{msm}) \left[\eta_{msm} \beta_M^M \frac{I_{msm}}{N_{msm}} + (1 - \eta_{msm}) \beta_F^M \frac{I_{hetf}}{N_{hetf}} \right] S_{msm} - (\mu + \delta_{msm}) I_{msm}, \\ \frac{dS_{hetf}}{dt} = \Pi_{hetf} - a_{hetf}(1 - \varepsilon_{hetf}) \beta_F^M \left[\alpha_{hetf} \frac{I_{msm}}{N_{msm}} + (1 - \alpha_{hetf}) \frac{I_{hetm}}{N_{hetm}} \right] S_{hetf} - \mu S_{hetf}, \\ \frac{dI_{hetf}}{dt} = a_{hetf}(1 - \varepsilon_{hetf}) \beta_F^M \left[\alpha_{hetf} \frac{I_{msm}}{N_{msm}} + (1 - \alpha_{hetf}) \frac{I_{hetm}}{N_{hetm}} \right] S_{hetf} - (\mu + \delta_{hetf}) I_{hetf}, \\ \frac{dS_{hetm}}{dt} = \Pi_{hetm} - a_{hetm}(1 - \varepsilon_{hetm}) \beta_F^M \frac{I_{hetf}}{N_{hetf}} S_{hetm} - \mu S_{hetm}, \\ \frac{dI_{hetm}}{dt} = a_{hetm}(1 - \varepsilon_{hetm}) \beta_F^M \frac{I_{hetf}}{N_{hetf}} S_{hetm} - (\mu + \delta_{hetm}) I_{hetm}, \end{array} \right. \quad (2.1)$$

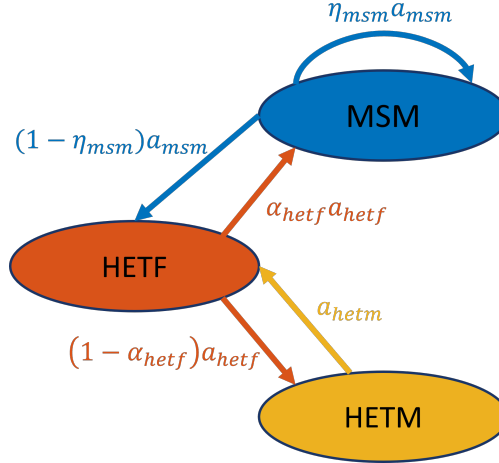


Figure 2.1: Sexual contact structure of the basic model (2.1).

State variable	Description
S_{msm}	Population of susceptible MSM
I_{msm}	Population of HIV-infected MSM
S_{hetf}	Population of susceptible HETF
I_{hetf}	Population of HIV-infected HETF
S_{hetm}	Population of susceptible HETM
I_{hetm}	Population of HIV-infected HETM

Table 1: Description of state variables of the basic model (2.1).

together with appropriate initial conditions. The descriptions of the state variables and parameters are tabulated in Tables 1 and 2, respectively.

Closure conditions must be satisfied to ensure that intra-group contacts are symmetric (as suggested by Figure 2.1); that is, the number of contacts HETF has with MSM (resp. HETF and HETM) are the same as the number of contacts MSM has with HETF (resp. HETM and HETF). Specifically:

$$(1 - \eta_{msm})N_{msm}a_{msm} = \alpha_{hetf}N_{hetf}a_{hetf} \quad \text{and} \quad (1 - \alpha_{hetf})N_{hetf}a_{hetf} = N_{hetm}a_{hetm}. \quad (2.2)$$

2.1 Mathematical analysis

In this section we explore the basic qualitative features of the model (2.1) with respect to its well-posedness, specifically, non-negativity and boundedness of solutions under suitable initial conditions. We also perform an analysis around the disease-free equilibrium to investigate the local and global stability properties of the model.

Parameter	Description
Π_j ($j = msm, hetf, hetm$)	Recruitment rate into the sexually-active population for group j
a_j ($j = msm, hetf, hetm$)	Average number of contacts per year for group j
δ_j ($j = msm, hetf, hetm$)	Disease-induced mortality rate for HIV-infected individuals in group j
ε_j ($j = msm, hetf, hetm$)	Fraction of individuals in group j who are on PrEP
μ	Natural death (or removal) rate in the community
β_M^M	Probability of HIV transmission per male-to-male contact
β_F^M	Probability of HIV transmission per female-to-male contact
β_M^F	Probability of HIV transmission per male-to-female contact
η_{msm}	Proportion of MSM contacts that are with MSM
α_{hetf}	Proportion of HETF contacts that are with MSM

Table 2: Description of parameters of the basic model (2.1).

We claim the following result:

Theorem 2.1. *Consider the basic model (2.1) with non-negative initial conditions. The region:*

$$\Omega = \left\{ (S_{msm}, I_{msm}, S_{hetf}, I_{hetf}, S_{hetm}, I_{hetm}) \in \mathbb{R}_+^6 : 0 \leq N \leq \frac{\Pi}{\mu} \right\}, \text{ where } \Pi = \Pi_{msm} + \Pi_{hetf} + \Pi_{hetm}$$

is positively-invariant and attracts all solutions of the model (2.1).

Proof. Adding all the equations of (2.1) gives:

$$\frac{dN}{dt} = \Pi - \mu N - \delta_{msm} I_{msm} - \delta_{hetf} I_{hetf} - \delta_{hetm} I_{hetm}.$$

Since all state variables and parameters of the model are non-negative, it follows that:

$$\frac{dN}{dt} \leq \Pi - \mu N. \quad (2.3)$$

Thus, by applying a standard comparison theorem [41] we obtain:

$$N(t) \leq \frac{\Pi}{\mu} + \left[N(0) - \frac{\Pi}{\mu} \right] e^{-\mu t}.$$

In particular, $N(t) \leq \frac{\Pi}{\mu}$ if $N(0) \leq \frac{\Pi}{\mu}$, i.e. every solution of the basic model (2.1) with initial conditions in Ω remains in Ω for all time. Furthermore, from (2.3) it follows that if $N(t) \geq \frac{\Pi}{\mu}$, then $\frac{dN}{dt} \leq 0$. In particular, this holds if $N(0) \geq \frac{\Pi}{\mu}$, which implies that Ω is attracting. \square

The consequence of Theorem 2.1 is that it is sufficient to consider the dynamics of the flow generated by the basic model (2.1) in Ω , where the model is well-posed mathematically and epidemiologically [42]; for this reason Ω may be referred to as the “biologically-feasible region”.

2.1.1 Local asymptotic stability of the disease-free equilibrium of the basic model

In this section, the asymptotic stability property of the disease-free equilibrium of the basic model (2.1) is explored. The disease-free equilibrium of the model (2.1), denoted as \mathcal{E}_0 , is given by:

$$\mathcal{E}_0 = (S_{msm}^*, I_{msm}^*, S_{hetf}^*, I_{hetf}^*, S_{hetm}^*, I_{hetm}^*) = \left(\frac{\Pi_{msm}}{\mu}, 0, \frac{\Pi_{hetf}}{\mu}, 0, \frac{\Pi_{hetm}}{\mu} \right). \quad (2.4)$$

The next generation operator method [43, 44] can then be used to analyze the local asymptotic stability property of \mathcal{E}_0 . Using the notation given in [43], the associated non-negative matrix of new infection terms F and the M-matrix of all linear transition terms V are given, respectively, by

$$F = \begin{bmatrix} f_{11} & f_{12} & 0 \\ f_{21} & 0 & f_{23} \\ 0 & f_{32} & 0 \end{bmatrix} \quad \text{and} \quad V = \begin{bmatrix} \mu + \delta_{msm} & 0 & 0 \\ 0 & \mu + \delta_{hetf} & 0 \\ 0 & 0 & \mu + \delta_{hetm} \end{bmatrix}, \quad (2.5)$$

where (noting that $N_{msm}^* = S_{msm}^*$, $N_{hetf}^* = S_{hetf}^*$, and $N_{hetm}^* = S_{hetm}^*$, see (2.4))

$$\begin{aligned} f_{11} &= \frac{[a_{msm} (1 - \varepsilon_{msm}) \eta_{msm} \beta_M^M] S_{msm}^*}{N_{msm}^*}, & f_{12} &= \frac{[a_{msm} (1 - \varepsilon_{msm}) (1 - \eta_{msm}) \beta_F^M] S_{msm}^*}{N_{hetf}^*}, \\ f_{21} &= \frac{[a_{hetf} (1 - \varepsilon_{hetf}) \alpha_{hetf} \beta_M^F] S_{hetf}^*}{N_{msm}^*}, & f_{23} &= \frac{[a_{hetf} (1 - \varepsilon_{hetf}) (1 - \alpha_{hetf}) \beta_M^F] S_{hetf}^*}{N_{hetm}^*}, \\ f_{32} &= \frac{[a_{hetm} (1 - \varepsilon_{hetm}) \beta_F^M] S_{hetm}^*}{N_{hetf}^*}. \end{aligned}$$

It is convenient to define the following quantity (where ρ is the spectral radius):

$$\mathbb{R}_c = \rho(FV^{-1}) = \frac{G_2}{G_1} + G_1 + \frac{G_{msm}^{msm}}{3}, \quad (2.6)$$

where,

$$G_1 = \left(\sqrt{(G_4 + G_3)^2 - G_2^3} + G_4 + G_3 \right)^{1/3}, \quad G_2 = \left(\frac{G_{msm}^{msm}}{3} \right)^2 + \frac{1}{3} G_{hetf}^{hetm} (G_{hetf}^{hetf} + G_{msm}^{hetf}),$$

$$G_3 = G_{msm}^{msm} \left(\frac{G_{msm}^{hetf} G_{hetf}^{msm}}{6} - \frac{2G_{hetf}^{hetm} G_{hetf}^{hetm}}{3} \right), \quad G_4 = \left(\frac{G_{msm}^{msm}}{3} \right)^3,$$

with,

$$G_{msm}^{msm} = \frac{f_{11}}{(\mu + \delta_{msm})}, \quad G_{hetf}^{msm} = \frac{f_{12} N_{hetf}^*}{(\mu + \delta_{hetf}) N_{msm}^*},$$

$$G_{msm}^{hetf} = \frac{f_{21} N_{msm}^*}{(\mu + \delta_{msm}) N_{hetf}^*}, \quad G_{hetm}^{hetf} = \frac{f_{23} N_{hetm}^*}{(\mu + \delta_{hetm}) N_{hetf}^*}, \quad G_{hetf}^{hetm} = \frac{f_{32} N_{hetf}^*}{(\mu + \delta_{hetf}) N_{hetm}^*}.$$

The quantity \mathbb{R}_c is the *control reproduction number* of the model. It measures the average number of new HIV cases generated by a typical HIV-infected individual if introduced in a population where a certain proportion of high-risk individuals are on PrEP [42, 45]. It should be noted from the expression (2.6) that the term G_{msm}^{msm} appears independently, signifying the fact that a significant portion of transmission dynamics in MSM occur independently of the other (HETF, HETM) risk groups. Thus, if the value of the entry f_{11} of the next generation matrix F is sufficiently large, HIV will persist in the population, regardless of the transmission levels in the other groups. Furthermore, it is noteworthy from the definitions of G_2 and G_3 that transmission between heterosexual individuals is heavily influenced by MSM dynamics. In particular, in G_2 , we observe a direct coupling between transmission from HETF to HETM and transmission from MSM to HETF. Finally, it can be seen from the expression for G_3 that a coupling exists between within-MSM transmission and transmission in the heterosexual populations. In other words, the above analysis suggests a significant coupling between HIV transmission in the MSM population and transmission within the heterosexual population, motivating detailed assessment of spillover effects between the high risk groups.

The result below follows from Theorem 2 of [43].

Theorem 2.2. *The disease-free equilibrium \mathcal{E}_0 of the model (2.1) is locally-asymptotically stable if $\mathbb{R}_c < 1$, and unstable if $\mathbb{R}_c > 1$.*

The epidemiological implication of Theorem 2.2 is that a small influx of HIV-infected individuals will not generate a large outbreak in the community if the quantity \mathbb{R}_c can be brought to (and maintained at) a value less than one. That is, the disease rapidly dies out or the community-level transmission of the disease can be controlled (when $\mathbb{R}_c < 1$) if the initial conditions are in the basin of attraction of the disease-free equilibrium.

2.1.2 Global asymptotic stability of the disease-free equilibrium: special case

In this section, we extend the result in Theorem 2.2 to prove the global asymptotic stability of the disease-free equilibrium for a special case of the model (2.1), namely, we consider $\delta_{msm} = \delta_{hetf} = \delta_{hetm} = 0$. This is a reasonable assumption; since HIV is lifelong, considering $\delta_j > 0$ reduces possible transmission time, and hence assuming $\delta_j = 0$ is conservative. To illustrate this point further, note that:

$$\frac{d}{d\delta_{msm}} [G_{msm}^{msm}] = -\frac{f_{11}}{(\mu + \delta_{msm})^2}.$$

Recalling that $f_{11} > 0$, we conclude that:

$$\frac{d}{d\delta_{msm}} [G_{msm}^{msm}] < 0,$$

implying that increased δ_{msm} can only serve to decrease G_{msm}^{msm} . Similar reasoning holds for the other G_j^i terms.

Furthermore, by adding the equations for the respective rate of change of sub-populations in the susceptible and infected compartments, we obtain

$$\frac{dN_j(t)}{dt} = \Pi_j - \mu N_j, \quad j = \{msm, hetf, hetm\}.$$

It thus follows that $N_j(t) \rightarrow \frac{\Pi_j}{\mu}$ as $t \rightarrow \infty$. From now on, the total sexually active population in group j at time t , denoted by $N_j(t)$, will be replaced by its limiting value, $N_j^* = \frac{\Pi_j}{\mu}$. In other words, the standard incidence formulation is now replaced by a mass action incidence.

Consider, now, the following feasible region for the special case of the basic model (2.1):

$$\Omega^* = \{(S_{msm}, I_{msm}, S_{hetf}, I_{hetf}, S_{hetm}, I_{hetm}) \in \Omega : S_{msm} \leq S_{msm}^*, S_{hetf} \leq S_{hetf}^*, S_{hetm} \leq S_{hetm}^*\}. \quad (2.7)$$

It can be shown that the region Ω^* is also positively-invariant and attracting with respect to this special case of the model (see Appendix A, Theorem A.1). It is convenient to define the following threshold quantity:

$$\widehat{\mathbb{R}}_c = \mathbb{R}_c|_{\delta_{msm}=\delta_{hetf}=\delta_{hetm}=0}.$$

We claim the following result (the proof of Theorem 2.3 is given in Appendix A):

Theorem 2.3. *The disease-free equilibrium \mathcal{E}_0 of the special case of the basic model (2.1) with $\delta_{msm} = \delta_{hetf} = \delta_{hetm} = 0$ is globally-asymptotically stable in Ω^* whenever $\widehat{\mathbb{R}}_c < 1$.*

The epidemiological implication of Theorem 2.3 is that, for the special case of the basic model (2.1) with negligible disease-induced mortality, HIV can be eliminated from the population if the PrEP-based intervention can bring (and maintain) the associated control reproduction number $\widehat{\mathbb{R}}_c$ to a value below one, regardless of the initial number of HIV-infected individuals in the population. Mathematically-speaking, $\widehat{\mathbb{R}}_c < 1$ is necessary and sufficient for the elimination of HIV in the community.

2.2 Qualitative analysis and assessment of PrEP spillover effects

The mixing structure of the model (2.1) raises important questions regarding the allocation of PrEP. In particular, we seek to better understand the spillover effects resulting from PrEP delivery to transmission groups. Such effects are observed in other group-structured models examining population mixing [26, 27], and modeling studies incorporating PrEP have also shown evidence of these effects [21, 24]. However, the mixing structure of (2.1), while seemingly simple, does not correspond to the well-understood cases of homogeneous or preferential (like-with-like) mixing (see e.g. [25, 26, 28, 29]). Analyzing spillover effects entails quantifying how PrEP uptake in one subgroup alters the incidence of the disease in the other subgroups. Thus, we consider the HIV *incidence* (i.e., average number of new infections *per unit time*) in group j at a time t , given by (assuming, as before, that $\delta_j = 0$ for simplicity):

$$\lambda_j(t) = \frac{dI_j}{dt} + \mu I_j \quad (2.8)$$

and aim at deriving system of equations that quantify its change in response to variations in PrEP allocation.

Note that linearization analysis, such as performed in the previous subsection, is inadequate to analyze PrEP spillover beyond a basic level. To understand why, consider the system (2.1), and assume we wish to study how incidence among HETF changes in response to increases in PrEP among MSM. Incidence for HETF λ_{hetf} is given by the equation:

$$\lambda_{hetf} = a_{hetf} (1 - \varepsilon_{hetf}) \beta_M^F \left[\alpha_{hetf} \frac{I_{msm}}{N_{msm}} + (1 - \alpha_{hetf}) \frac{I_{hetm}}{N_{hetm}} \right] S_{hetf}.$$

Changing PrEP among MSM affects the term I_{msm}/N_{msm} above; however, in a linearization analysis, this term, which is time-variant and depends on the current state of the MSM population (including PrEP use), must be *fixed* at a given point. Therefore, such techniques will not properly account for the influence of PrEP uptake among MSM on HETF incidence, particularly over longer time horizons.

We must therefore apply a different approach to analyze the PrEP spillover effect. In particular, we define the following two auxiliary quantities:

$$\sigma_j^k(t) := \frac{dS_j}{d\varepsilon_k}, \quad \gamma_j^k(t) := \frac{dI_j}{d\varepsilon_k}, \quad (2.9)$$

which describe the response in a group j to a change in the *fraction* of individuals on PrEP ε_k in group k . For example, we can view γ_{msm}^{msm} as defining the *direct effect* of PrEP use among MSM on MSM incidence, while γ_{hetf}^{msm} and γ_{hetm}^{msm} give the *spillover effect* of PrEP use among MSM on HETF and HETM incidence, respectively.

However, for most intervention applications, including those studied herein, the *number of individuals on PrEP* in a population E_k , not the fraction, is more relevant. One can modify (2.9) in a straightforward way by observing that the fraction of PrEP users can be written as:

$$\varepsilon_k = \frac{E_k}{S_k}. \quad (2.10)$$

Then, applying the chain rule gives:

$$\frac{\partial S_j}{\partial E_k} = \frac{\partial S_j}{\partial \varepsilon_k} \times \frac{d\varepsilon_k}{dE_k} = \frac{\sigma_j^k}{S_k}, \quad \frac{\partial I_j}{\partial E_k} = \frac{\partial I_j}{\partial \varepsilon_k} \times \frac{d\varepsilon_k}{dE_k} = \frac{\gamma_j^k}{S_k}, \quad (2.11)$$

which describe the response of S_j , I_j to the *number* of PrEP users in group k , rather than the fraction. Indeed, in the sections that follow, we will be primarily concerned with this quantity.

The sensitivity of (2.8) on PrEP uptake is obtained as:

$$\frac{\partial}{\partial E_k} [\lambda_j(t)] = \frac{\partial}{\partial E_k} \left[\frac{dI_j}{dt} \right] + \mu \frac{\partial}{\partial E_k} [I_j] = \frac{d}{dt} \left[\frac{\partial I_j}{\partial E_k} \right] + \mu \frac{\gamma_j^k}{S_k} = \frac{d}{dt} \left[\frac{\gamma_j^k}{S_k} \right] + \mu \frac{\gamma_j^k}{S_k}. \quad (2.12)$$

Note that γ_j^k/S_k has units (New infections) / (Additional Person on PrEP). It follows that S_k/γ_j^k has units (Additional Person on PrEP) / (New Infections). This motivates the following proposition, relating the quantities (2.11) to the *Number Needed to Treat* (NNT), the primary quantity used to measure PrEP effectiveness in population-wide studies of PrEP [33, 34, 35, 19], defined as:

$$\text{NNT} = \frac{\text{Number of additional person-years on PrEP}}{\text{Number of HIV infections prevented}}. \quad (2.13)$$

Note that the use of person-years in the numerator of (2.13) implicitly introduces time-dependence.

Proposition 2.4. *The number needed to treat (NNT), interpreted as the number of additional PrEP users (in person-years) necessary to prevent an additional HIV infection over a time period $[0, T]$, can be approximated as:*

$$\text{NNT}(T) \approx T \frac{S_k(T)}{\gamma_j^k(T)}. \quad (2.14)$$

Proof. Assume initially that there are E_k^0 total PrEP users in group k , and let ΔE_k denote an increment of additional PrEP users in group k . Denote as $\lambda_j(\hat{E}_0)$ the original incidence in group j , and $\lambda_j(E_k^0 + \Delta E_k)$ the incidence in group j after increasing the number of PrEP users in group k by ΔE_k .

From the NNT formula (2.13) we get:

$$\text{NNT} = \frac{T \Delta E_k}{\int_0^T \lambda_j(E_k^0) - \lambda_j(E_k^0 + \Delta E_k) dt}. \quad (2.15)$$

We now expand $\lambda_j(E_k^0 + \Delta E_k)$ in a Taylor series about E_k^0 , giving:

$$\lambda_j(E_k^0 + \Delta E_k) = \lambda_j(E_k^0) + \frac{\partial}{\partial E_k} [\lambda_j(E_k^0)] \Delta E_k + \mathcal{O}(\Delta E_k^2) \quad (2.16)$$

Neglecting higher-order terms, substituting (2.16) into (2.15) gives:

$$\text{NNT} \approx \frac{T \Delta E_k}{\int_0^T \left(\lambda_j(E_k^0) - \left(\lambda_j(E_k^0) + \frac{\partial}{\partial E_k} [\lambda_j(E_k^0)] \Delta E_k \right) \right) dt} = \frac{T}{\int_0^T \frac{\partial}{\partial E_k} [\lambda_j(E_k^0)] dt}. \quad (2.17)$$

Recalling (2.12), we may write (2.17) as:

$$\text{NNT} \approx \frac{T}{\int_0^T \left(\frac{d}{dt} \left[\frac{\gamma_j^k}{S_k} \right] + \mu \frac{\gamma_j^k}{S_k} \right) dt} = \frac{T}{\int_0^T e^{-\mu t} \frac{d}{dt} \left[\frac{\gamma_j^k}{S_k} e^{\mu t} \right] dt}.$$

Evaluating the integral in the denominator yields:

$$\int_0^T e^{-\mu t} \frac{d}{dt} \left[\frac{\gamma_j^k}{S_k} e^{\mu t} \right] dt = \left[e^{-\mu t} e^{\mu t} \frac{\gamma_j^k(t)}{S_k(t)} \right]_0^T + \mu \int_0^T \frac{\gamma_j^k}{S_k} dt. \quad (2.18)$$

Noting that $\gamma_j^k(0) = 0$, we obtain:

$$\text{NNT} \approx \frac{T}{\frac{\gamma_j^k(T)}{S_k(T)} + \mu \int_0^T \frac{\gamma_j^k}{S_k} dt}. \quad (2.19)$$

In general, the mortality rate μ corresponds to much longer time-scales than the simulation period $[0, T]$ (in this work we have $\mu = 1/50$ years compared to a 10-year simulation period, see Section 2.3). Hence, over shorter time scales, we may neglect the integral term in the denominator (2.19), obtaining:

$$\text{NNT}(T) \approx T \frac{S_k(T)}{\gamma_j^k(T)},$$

which was to be shown. \square

2.2.1 Spillover equation derivation

The goal of this section is to derive differential equations for (2.9) that enter in the expression describing the sensitivity on PrEP uptake given in (2.12). We begin by considering the system (2.1) with the simplifying assumption that $\delta_j = 0$ for each group. The reason for this will become clear later. Let us start by introducing the following notation:

$$\begin{aligned} \mathbf{X} &= \begin{pmatrix} S_{msm} \\ I_{msm} \\ S_{hetf} \\ I_{hetf} \\ S_{hetm} \\ I_{hetm} \end{pmatrix}, \quad \mathbf{\Lambda}_{msm} = \begin{pmatrix} 0 \\ a_{msm} \eta_{msm} \frac{\beta_M^M}{N_{msm}} \\ 0 \\ a_{msm} (1 - \eta_{msm}) \frac{\beta_F^M}{N_{hetf}} \\ 0 \\ 0 \end{pmatrix}, \\ \mathbf{\Lambda}_{hetf} &= \begin{pmatrix} 0 \\ a_{hetf} \alpha_{hetf} \frac{\beta_M^F}{N_{msm}} \\ 0 \\ 0 \\ 0 \\ a_{hetf} (1 - \alpha_{hetf}) \frac{\beta_F^M}{N_{hetm}} \end{pmatrix}, \quad \mathbf{\Lambda}_{hetm} = \begin{pmatrix} 0 \\ 0 \\ 0 \\ a_{hetm} \frac{\beta_F^M}{N_{hetf}} \\ 0 \\ 0 \end{pmatrix} \end{aligned} \quad (2.20)$$

such that we can write the system (2.1) more compactly as:

$$\left\{ \begin{aligned} \frac{dS_{msm}}{dt} &= \Pi_{msm} - (1 - \varepsilon_{msm}) \left(\mathbf{\Lambda}_{msm}^T \mathbf{X} \right) S_{msm} - \mu S_{msm}, \\ \frac{dI_{msm}}{dt} &= (1 - \varepsilon_{msm}) \left(\mathbf{\Lambda}_{msm}^T \mathbf{X} \right) S_{msm} - \mu I_{msm}, \\ \frac{dS_{hetf}}{dt} &= \Pi_{hetf} - (1 - \varepsilon_{hetf}) \left(\mathbf{\Lambda}_{hetf}^T \mathbf{X} \right) S_{hetf} - \mu S_{hetf}, \\ \frac{dI_{hetf}}{dt} &= (1 - \varepsilon_{hetf}) \left(\mathbf{\Lambda}_{hetf}^T \mathbf{X} \right) S_{hetf} - \mu I_{hetf}, \\ \frac{dS_{hetm}}{dt} &= \Pi_{hetm} - (1 - \varepsilon_{hetm}) \left(\mathbf{\Lambda}_{hetm}^T \mathbf{X} \right) S_{hetm} - \mu S_{hetm}, \\ \frac{dI_{hetm}}{dt} &= (1 - \varepsilon_{hetm}) \left(\mathbf{\Lambda}_{hetm}^T \mathbf{X} \right) S_{hetm} - \mu I_{hetm}. \end{aligned} \right. \quad (2.21)$$

Let us then introduce a perturbation $\tilde{\varepsilon}$ to the PrEP fraction among MSM, denoting the resulting perturbed quantities as \widehat{S}_j , \widehat{I}_j , $\widehat{\mathbf{X}}$. The perturbed system reads:

$$\left\{ \begin{array}{l} \frac{d\widehat{S}_{msm}}{dt} = \Pi_{msm} - (1 - (\varepsilon_{msm} + \tilde{\varepsilon})) \left(\mathbf{\Lambda}_{msm}^T \widehat{\mathbf{X}} \right) \widehat{S}_{msm} - \mu \widehat{S}_{msm}, \\ \frac{d\widehat{I}_{msm}}{dt} = (1 - (\varepsilon_{msm} + \tilde{\varepsilon})) \left(\mathbf{\Lambda}_{msm}^T \widehat{\mathbf{X}} \right) \widehat{S}_{msm} - \mu \widehat{I}_{msm}, \\ \frac{d\widehat{S}_{hetf}}{dt} = \Pi_{hetf} - (1 - \varepsilon_{hetf}) \left(\mathbf{\Lambda}_{hetf}^T \widehat{\mathbf{X}} \right) \widehat{S}_{hetf} - \mu \widehat{S}_{hetf}, \\ \frac{d\widehat{I}_{hetf}}{dt} = (1 - \varepsilon_{hetf}) \left(\mathbf{\Lambda}_{hetf}^T \widehat{\mathbf{X}} \right) \widehat{S}_{hetf} - \mu \widehat{I}_{hetf}, \\ \frac{d\widehat{S}_{hetm}}{dt} = \Pi_{hetm} - (1 - \varepsilon_{hetm}) \left(\mathbf{\Lambda}_{hetm}^T \widehat{\mathbf{X}} \right) \widehat{S}_{hetm} - \mu \widehat{S}_{hetm}, \\ \frac{d\widehat{I}_{hetm}}{dt} = (1 - \varepsilon_{hetm}) \left(\mathbf{\Lambda}_{hetm}^T \widehat{\mathbf{X}} \right) \widehat{S}_{hetm} - \mu \widehat{I}_{hetm}. \end{array} \right. \quad (2.22)$$

Note that the $\mathbf{\Lambda}_j$ is the same in (2.21) and (2.22) for all time t . To see this, note from (2.20) that the only state-dependent terms in the $\mathbf{\Lambda}_j$ are the total population denominators N_j . Adding a generic S_j and I_j compartment in (2.21), one obtains the following differential equation for N_j :

$$\frac{dN_j}{dt} = \Pi_j - \mu S_j - \mu I_j = \Pi_j - \mu N_j. \quad (2.23)$$

Similarly, for (2.22),

$$\frac{d\widehat{N}_j}{dt} = \Pi_j - \mu \widehat{S}_j - \mu \widehat{I}_j = \Pi_j - \mu \widehat{N}_j. \quad (2.24)$$

Hence, if $N_j(0) = \widehat{N}_j(0)$, we have that $N_j(t) = \widehat{N}_j(t)$ at all time.

We remark that, in the case where $\delta_j \neq 0$, $N_j(t) = \widehat{N}_j(t)$ no longer holds. In such a case, (2.23)-(2.24) instead become:

$$\frac{dN_j}{dt} = \Pi_j - \mu S_j - (\mu + \delta_j) I_j = \Pi_j - \mu N_j - \delta_j I_j, \quad (2.25)$$

and

$$\frac{d\widehat{N}_j}{dt} = \Pi_j - \mu \widehat{S}_j - (\mu + \delta_j) \widehat{I}_j = \Pi_j - \mu \widehat{N}_j - \delta_j \widehat{I}_j. \quad (2.26)$$

Even if $N_j(0) = \widehat{N}_j(0)$, from (2.23)-(2.24), it follows that $N_j(t) \neq \widehat{N}_j(t)$ when $I_j(t) \neq \widehat{I}_j(t)$, which is the case in general, as PrEP leads to reduced HIV incidence.

In other words, for $\delta_j = 0$, even if $\widehat{S}_j(t) \neq S_j(t)$, $\widehat{I}_j(t) \neq I_j(t)$, we nonetheless have that $N_j(t) = \widehat{N}_j(t)$. In practice, differences in the N_j populations arising from $\delta_j \neq 0$ are insignificant as $S_j \gg I_j$, $\Pi_j \gg \delta_j I_j$. Nevertheless, it is possible to relax the assumption that $\delta_j = 0$, though the resulting analysis is more complex; we provide this information to the interested reader in Appendix B.

Next, assuming identical initial conditions in both (2.21), (2.22) and subtracting (2.21) from (2.22) gives:

$$\left\{ \begin{array}{l} \frac{d(\widehat{S_{msm}} - S_{msm})}{dt} = -(1 - \varepsilon_{msm}) \left(\mathbf{\Lambda}_{msm}^T \widehat{\mathbf{X}} \right) \widehat{S_{msm}} + \tilde{\varepsilon} \left(\mathbf{\Lambda}_{msm}^T \widehat{\mathbf{X}} \right) \widehat{S_{msm}} \\ \quad + (1 - \varepsilon_{msm}) \left(\mathbf{\Lambda}_{msm}^T \mathbf{X} \right) S_{msm} - \mu \left(\widehat{S_{msm}} - S_{msm} \right), \\ \frac{d(\widehat{I_{msm}} - I_{msm})}{dt} = (1 - \varepsilon_{msm}) \left(\mathbf{\Lambda}_{msm}^T \widehat{\mathbf{X}} \right) \widehat{S_{msm}} - \tilde{\varepsilon} \left(\mathbf{\Lambda}_{msm}^T \widehat{\mathbf{X}} \right) \widehat{S_{msm}} \\ \quad - (1 - \varepsilon_{msm}) \left(\mathbf{\Lambda}_{msm}^T \mathbf{X} \right) S_{msm} - \mu \left(\widehat{I_{msm}} - I_{msm} \right), \\ \frac{d(\widehat{S_{hetf}} - S_{hetf})}{dt} = -(1 - \varepsilon_{hetf}) \left(\mathbf{\Lambda}_{hetf}^T \widehat{\mathbf{X}} \right) \widehat{S_{hetf}} + (1 - \varepsilon_{hetf}) \left(\mathbf{\Lambda}_{hetf}^T \mathbf{X} \right) S_{hetf} \\ \quad - \mu \left(\widehat{S_{hetf}} - S_{hetf} \right), \\ \frac{d(\widehat{I_{hetf}} - I_{hetf})}{dt} = (1 - \varepsilon_{hetf}) \left(\mathbf{\Lambda}_{hetf}^T \widehat{\mathbf{X}} \right) \widehat{S_{hetf}} - (1 - \varepsilon_{hetf}) \left(\mathbf{\Lambda}_{hetf}^T \mathbf{X} \right) S_{hetf} \\ \quad - \mu \left(\widehat{I_{hetf}} - I_{hetf} \right), \\ \frac{d(\widehat{S_{hetm}} - S_{hetm})}{dt} = -(1 - \varepsilon_{hetm}) \left(\mathbf{\Lambda}_{hetm}^T \widehat{\mathbf{X}} \right) \widehat{S_{hetm}} + (1 - \varepsilon_{hetm}) \left(\mathbf{\Lambda}_{hetm}^T \mathbf{X} \right) S_{hetm} \\ \quad - \mu \left(\widehat{S_{hetm}} - S_{hetm} \right), \\ \frac{d(\widehat{I_{hetm}} - I_{hetm})}{dt} = (1 - \varepsilon_{hetm}) \left(\mathbf{\Lambda}_{hetm}^T \widehat{\mathbf{X}} \right) \widehat{S_{hetm}} - (1 - \varepsilon_{hetm}) \left(\mathbf{\Lambda}_{hetm}^T \mathbf{X} \right) S_{hetm} \\ \quad - \mu \left(\widehat{I_{hetm}} - I_{hetm} \right) \end{array} \right. \quad (2.27)$$

with zero initial conditions. To aid later manipulations, we add productive zeros to obtain the following identity:

$$\begin{aligned} & - \left(\mathbf{\Lambda}_j^T \widehat{\mathbf{X}} \right) \widehat{S}_j + \left(\mathbf{\Lambda}_j^T \mathbf{X} \right) S_j \\ & = - \left(\mathbf{\Lambda}_j^T \left(\widehat{\mathbf{X}} - \mathbf{X} + \mathbf{X} \right) \right) \left(\widehat{S}_j - S_j + S_j \right) + \left(\mathbf{\Lambda}_j^T \mathbf{X} \right) S_j \\ & = - \left(\mathbf{\Lambda}_j^T \left(\widehat{\mathbf{X}} - \mathbf{X} \right) \right) \left(\widehat{S}_j - S_j \right) - \left(\mathbf{\Lambda}_j^T \widehat{\mathbf{X}} \right) \left(\widehat{S}_j - S_j \right) - \left(\mathbf{\Lambda}_j^T \left(\widehat{\mathbf{X}} - \mathbf{X} \right) \right) \widehat{S}_j. \end{aligned} \quad (2.28)$$

Applying (2.28) to (2.27) yields:

$$\left\{ \begin{array}{l} \frac{d(\widehat{S}_{msm} - S_{msm})}{dt} = -(1 - \varepsilon_{msm}) \left[\left(\mathbf{\Lambda}_{msm}^T (\widehat{\mathbf{X}} - \mathbf{X}) \right) (\widehat{S}_{msm} - S_{msm}) + \left(\mathbf{\Lambda}_{msm}^T (\widehat{\mathbf{X}} - \mathbf{X}) \right) \widehat{S}_{msm} \right. \\ \quad \left. + \left(\mathbf{\Lambda}_{msm}^T \widehat{\mathbf{X}} \right) (\widehat{S}_{msm} - S_{msm}) \right] + \tilde{\varepsilon} \left(\mathbf{\Lambda}_{msm}^T \widehat{\mathbf{X}} \right) \widehat{S}_{msm} - \mu (\widehat{S}_{msm} - S_{msm}), \\ \frac{d(\widehat{I}_{msm} - I_{msm})}{dt} = (1 - \varepsilon_{msm}) \left[\left(\mathbf{\Lambda}_{msm}^T (\widehat{\mathbf{X}} - \mathbf{X}) \right) (\widehat{S}_{msm} - S_{msm}) + \left(\mathbf{\Lambda}_{msm}^T (\widehat{\mathbf{X}} - \mathbf{X}) \right) \widehat{S}_{msm} \right. \\ \quad \left. + \left(\mathbf{\Lambda}_{msm}^T \widehat{\mathbf{X}} \right) (\widehat{S}_{msm} - S_{msm}) \right] - \tilde{\varepsilon} \left(\mathbf{\Lambda}_{msm}^T \widehat{\mathbf{X}} \right) \widehat{S}_{msm} - \mu (\widehat{I}_{msm} - I_{msm}), \\ \frac{d(\widehat{S}_{hetf} - S_{hetf})}{dt} = -(1 - \varepsilon_{hetf}) \left[\left(\mathbf{\Lambda}_{hetf}^T (\widehat{\mathbf{X}} - \mathbf{X}) \right) (\widehat{S}_{hetf} - S_{hetf}) + \left(\mathbf{\Lambda}_{hetf}^T (\widehat{\mathbf{X}} - \mathbf{X}) \right) \widehat{S}_{hetf} \right. \\ \quad \left. + \left(\mathbf{\Lambda}_{hetf}^T \widehat{\mathbf{X}} \right) (\widehat{S}_{hetf} - S_{hetf}) \right] - \mu (\widehat{S}_{hetf} - S_{hetf}), \\ \frac{d(\widehat{I}_{hetf} - I_{hetf})}{dt} = (1 - \varepsilon_{hetf}) \left[\left(\mathbf{\Lambda}_{hetf}^T (\widehat{\mathbf{X}} - \mathbf{X}) \right) (\widehat{S}_{hetf} - S_{hetf}) + \left(\mathbf{\Lambda}_{hetf}^T (\widehat{\mathbf{X}} - \mathbf{X}) \right) \widehat{S}_{hetf} \right. \\ \quad \left. + \left(\mathbf{\Lambda}_{hetf}^T \widehat{\mathbf{X}} \right) (\widehat{S}_{hetf} - S_{hetf}) \right] - \mu (\widehat{I}_{hetf} - I_{hetf}), \\ \frac{d(\widehat{S}_{hetm} - S_{hetm})}{dt} = -(1 - \varepsilon_{hetm}) \left[\left(\mathbf{\Lambda}_{hetm}^T (\widehat{\mathbf{X}} - \mathbf{X}) \right) (\widehat{S}_{hetm} - S_{hetm}) + \left(\mathbf{\Lambda}_{hetm}^T (\widehat{\mathbf{X}} - \mathbf{X}) \right) \widehat{S}_{hetm} \right. \\ \quad \left. + \left(\mathbf{\Lambda}_{hetm}^T \widehat{\mathbf{X}} \right) (\widehat{S}_{hetm} - S_{hetm}) \right] - \mu (\widehat{S}_{hetm} - S_{hetm}), \\ \frac{d(\widehat{I}_{hetm} - I_{hetm})}{dt} = (1 - \varepsilon_{hetm}) \left[\left(\mathbf{\Lambda}_{hetm}^T (\widehat{\mathbf{X}} - \mathbf{X}) \right) (\widehat{S}_{hetm} - S_{hetm}) + \left(\mathbf{\Lambda}_{hetm}^T (\widehat{\mathbf{X}} - \mathbf{X}) \right) \widehat{S}_{hetm} \right. \\ \quad \left. + \left(\mathbf{\Lambda}_{hetm}^T \widehat{\mathbf{X}} \right) (\widehat{S}_{hetm} - S_{hetm}) \right] - \mu (\widehat{I}_{hetm} - I_{hetm}). \end{array} \right. \quad (2.29)$$

To obtain the expression in (2.9) we divide the equations in (2.29) by $\tilde{\varepsilon}$. To elucidate this point, we consider the first equation in (2.29) explicitly. Dividing by $\tilde{\varepsilon}$ gives:

$$\frac{d}{dt} \left[\frac{(\widehat{S}_{msm} - S_{msm})}{\tilde{\varepsilon}} \right] = -(1 - \varepsilon_{msm}) \left[\left(\mathbf{\Lambda}_{msm}^T \left(\frac{\widehat{\mathbf{X}} - \mathbf{X}}{\tilde{\varepsilon}} \right) \right) (\widehat{S}_{msm} - S_{msm}) + \left(\mathbf{\Lambda}_{msm}^T \left(\frac{\widehat{\mathbf{X}} - \mathbf{X}}{\tilde{\varepsilon}} \right) \right) \widehat{S}_{msm} \right. \\ \left. + \left(\mathbf{\Lambda}_{msm}^T \widehat{\mathbf{X}} \right) \left(\frac{\widehat{S}_{msm} - S_{msm}}{\tilde{\varepsilon}} \right) \right] + \left(\mathbf{\Lambda}_{msm}^T \widehat{\mathbf{X}} \right) \widehat{S}_{msm} - \mu \left(\frac{\widehat{S}_{msm} - S_{msm}}{\tilde{\varepsilon}} \right).$$

Further, we introduce the following notation

$$\boldsymbol{\vartheta}^{msm} = \lim_{\tilde{\varepsilon} \rightarrow 0} \frac{\widehat{\mathbf{X}} - \mathbf{X}}{\tilde{\varepsilon}} = \begin{pmatrix} \sigma_{msm}^{msm} \\ \gamma_{msm}^{msm} \\ \sigma_{hetf}^{msm} \\ \gamma_{hetf}^{msm} \\ \sigma_{hetm}^{msm} \\ \gamma_{hetm}^{msm} \end{pmatrix}$$

Then, taking the limit as $\tilde{\varepsilon} \rightarrow 0$ in the above equation and noting that $\widehat{\mathbf{X}} \rightarrow \mathbf{X}$, and $\widehat{S}_{msm} \rightarrow S_{msm}$ as $\tilde{\varepsilon} \rightarrow 0$, we obtain:

$$\frac{d\sigma_{msm}^{msm}}{dt} = -(1 - \varepsilon_{msm}) \left[\left(\mathbf{\Lambda}_{msm}^T \boldsymbol{\vartheta}^{msm} \right) S_{msm} + \left(\mathbf{\Lambda}_{msm}^T \mathbf{X} \right) \sigma_{msm}^{msm} \right] + \left(\mathbf{\Lambda}_{msm}^T \mathbf{X} \right) S_{msm} - \mu \sigma_{msm}^{msm}.$$

Proceeding analogously on the other equations in (2.29), we obtain the full system describing the effect of ε_{msm} on each compartment:

$$\left\{ \begin{array}{l} \frac{d\sigma_{msm}^{msm}}{dt} = -(1 - \varepsilon_{msm}) [(\Lambda_{msm}^T \vartheta^{msm}) S_{msm} + (\Lambda_{msm}^T \mathbf{X}) \sigma_{msm}^{msm}] + (\Lambda_{msm}^T \mathbf{X}) S_{msm} - \mu \sigma_{msm}^{msm}, \\ \frac{d\gamma_{msm}^{msm}}{dt} = (1 - \varepsilon_{msm}) [(\Lambda_{msm}^T \vartheta^{msm}) S_{msm} + (\Lambda_{msm}^T \mathbf{X}) \sigma_{msm}^{msm}] - (\Lambda_{msm}^T \mathbf{X}) S_{msm} - \mu \gamma_{msm}^{msm}, \\ \frac{d\sigma_{hetf}^{msm}}{dt} = -(1 - \varepsilon_{hetf}) [(\Lambda_{hetf}^T \vartheta^{msm}) S_{hetf} + (\Lambda_{hetf}^T \mathbf{X}) \sigma_{hetf}^{msm}] - \mu \sigma_{hetf}^{msm}, \\ \frac{d\gamma_{hetf}^{msm}}{dt} = (1 - \varepsilon_{hetf}) [(\Lambda_{hetf}^T \vartheta^{msm}) S_{hetf} + (\Lambda_{hetf}^T \mathbf{X}) \sigma_{hetf}^{msm}] - \mu \gamma_{hetf}^{msm}, \\ \frac{d\sigma_{hetm}^{msm}}{dt} = -(1 - \varepsilon_{hetm}) [(\Lambda_{hetm}^T \vartheta^{msm}) S_{hetm} + (\Lambda_{hetm}^T \mathbf{X}) \sigma_{hetm}^{msm}] - \mu \sigma_{hetm}^{msm}, \\ \frac{d\gamma_{hetm}^{msm}}{dt} = (1 - \varepsilon_{hetm}) [(\Lambda_{hetm}^T \vartheta^{msm}) S_{hetm} + (\Lambda_{hetm}^T \mathbf{X}) \sigma_{hetm}^{msm}] - \mu \gamma_{hetm}^{msm}. \end{array} \right. \quad (2.30)$$

Note that the initial conditions of the system (2.30) are zero in each equation. Applying an identical argument, but perturbing ε_{hetf} instead of ε_{msm} gives the system:

$$\left\{ \begin{array}{l} \frac{d\sigma_{msm}^{hetf}}{dt} = -(1 - \varepsilon_{msm}) [(\Lambda_{msm}^T \vartheta^{hetf}) S_{msm} + (\Lambda_{msm}^T \mathbf{X}) \sigma_{msm}^{hetf}] - \mu \sigma_{msm}^{hetf}, \\ \frac{d\gamma_{msm}^{hetf}}{dt} = (1 - \varepsilon_{msm}) [(\Lambda_{msm}^T \vartheta^{hetf}) S_{msm} + (\Lambda_{msm}^T \mathbf{X}) \sigma_{msm}^{hetf}] - \mu \gamma_{msm}^{hetf}, \\ \frac{d\sigma_{hetf}^{hetf}}{dt} = -(1 - \varepsilon_{hetf}) [(\Lambda_{hetf}^T \vartheta^{hetf}) S_{hetf} + (\Lambda_{hetf}^T \mathbf{X}) \sigma_{hetf}^{hetf}] + (\Lambda_{hetf}^T \mathbf{X}) S_{hetf} - \mu \sigma_{hetf}^{hetf}, \\ \frac{d\gamma_{hetf}^{hetf}}{dt} = (1 - \varepsilon_{hetf}) [(\Lambda_{hetf}^T \vartheta^{hetf}) S_{hetf} + (\Lambda_{hetf}^T \mathbf{X}) \sigma_{hetf}^{hetf}] - (\Lambda_{hetf}^T \mathbf{X}) S_{hetf} - \mu \gamma_{hetf}^{hetf}, \\ \frac{d\sigma_{hetm}^{hetf}}{dt} = -(1 - \varepsilon_{hetm}) [(\Lambda_{hetm}^T \vartheta^{hetf}) S_{hetm} + (\Lambda_{hetm}^T \mathbf{X}) \sigma_{hetm}^{hetf}] - \mu \sigma_{hetm}^{hetf}, \\ \frac{d\gamma_{hetm}^{hetf}}{dt} = (1 - \varepsilon_{hetm}) [(\Lambda_{hetm}^T \vartheta^{hetf}) S_{hetm} + (\Lambda_{hetm}^T \mathbf{X}) \sigma_{hetm}^{hetf}] - \mu \gamma_{hetm}^{hetf}, \end{array} \right. \quad (2.31)$$

which describes the effect of PrEP use among HETF. Finally, the system describing the effect of PrEP use among HETM on (2.21) reads:

$$\left\{ \begin{array}{l} \frac{d\sigma_{msm}^{hetm}}{dt} = -(1 - \varepsilon_{msm}) [(\Lambda_{msm}^T \vartheta^{hetm}) S_{msm} + (\Lambda_{msm}^T \mathbf{X}) \sigma_{msm}^{hetm}] - \mu \sigma_{msm}^{hetm}, \\ \frac{d\gamma_{msm}^{hetm}}{dt} = (1 - \varepsilon_{msm}) [(\Lambda_{msm}^T \vartheta^{hetm}) S_{msm} + (\Lambda_{msm}^T \mathbf{X}) \sigma_{msm}^{hetm}] - \mu \gamma_{msm}^{hetm}, \\ \frac{d\sigma_{hetf}^{hetm}}{dt} = -(1 - \varepsilon_{hetf}) [(\Lambda_{hetf}^T \vartheta^{hetm}) S_{hetf} + (\Lambda_{hetf}^T \mathbf{X}) \sigma_{hetf}^{hetm}] - \mu \sigma_{hetf}^{hetm}, \\ \frac{d\gamma_{hetf}^{hetm}}{dt} = (1 - \varepsilon_{hetf}) [(\Lambda_{hetf}^T \vartheta^{hetm}) S_{hetf} + (\Lambda_{hetf}^T \mathbf{X}) \sigma_{hetf}^{hetm}] - \mu \gamma_{hetf}^{hetm}, \\ \frac{d\sigma_{hetm}^{hetm}}{dt} = -(1 - \varepsilon_{hetm}) [(\Lambda_{hetm}^T \vartheta^{hetm}) S_{hetm} + (\Lambda_{hetm}^T \mathbf{X}) \sigma_{hetm}^{hetm}] + (\Lambda_{hetm}^T \mathbf{X}) S_{hetm} - \mu \sigma_{hetm}^{hetm}, \\ \frac{d\gamma_{hetm}^{hetm}}{dt} = (1 - \varepsilon_{hetm}) [(\Lambda_{hetm}^T \vartheta^{hetm}) S_{hetm} + (\Lambda_{hetm}^T \mathbf{X}) \sigma_{hetm}^{hetm}] - (\Lambda_{hetm}^T \mathbf{X}) S_{hetm} - \mu \gamma_{hetm}^{hetm}. \end{array} \right. \quad (2.32)$$

Together, we refer to the systems (2.30), (2.31), (2.32) as the *PrEP spillover equations*.

Remark 2.5. Note that the systems (2.30), (2.31), (2.32) are defined for specific values of ε_k (this is indeed a local analysis). We therefore expect the solution of the spillover systems to change when the value of ε_k is varied. Given current levels of PrEP usage remain quite low, we do not expect this to be a significant factor for examined values of ε_k . However, it may become more relevant in the coming years if PrEP uptake rates increase.

2.2.2 System for MSM in the original variables

For completeness, below we write the system (2.30) using the original variables/notation (2.1):

$$\left\{ \begin{array}{l} \frac{d\sigma_{msm}^{msm}}{dt} = -a_{msm}(1 - \varepsilon_{msm}) \left[\eta_{msm} \beta_M^M \frac{\gamma_{msm}}{N_{msm}} + (1 - \eta_{msm}) \beta_F^M \frac{\gamma_{hetf}}{N_{hetf}} \right] S_{msm} \\ \quad - a_{msm}(1 - \varepsilon_{msm}) \left[\eta_{msm} \beta_M^M \frac{I_{msm}}{N_{msm}} + (1 - \eta_{msm}) \beta_F^M \frac{I_{hetf}}{N_{hetf}} \right] \sigma_{msm}^{msm} \\ \quad + a_{msm} \left(\eta_{msm} \beta_M^M \frac{I_{msm}}{N_{msm}} + (1 - \eta_{msm}) \beta_F^M \frac{I_{hetf}}{N_{hetf}} \right) S_{msm} - \mu \sigma_{msm}^{msm}, \\ \frac{d\gamma_{msm}^{msm}}{dt} = a_{msm}(1 - \varepsilon_{msm}) \left[\eta_{msm} \beta_M^M \frac{\gamma_{msm}}{N_{msm}} + (1 - \eta_{msm}) \beta_F^M \frac{\gamma_{hetf}}{N_{hetf}} \right] S_{msm} \\ \quad + a_{msm}(1 - \varepsilon_{msm}) \left[\eta_{msm} \beta_M^M \frac{I_{msm}}{N_{msm}} + (1 - \eta_{msm}) \beta_F^M \frac{I_{hetf}}{N_{hetf}} \right] \sigma_{msm}^{msm} \\ \quad - a_{msm} \left(\eta_{msm} \beta_M^M \frac{I_{msm}}{N_{msm}} + (1 - \eta_{msm}) \beta_F^M \frac{I_{hetf}}{N_{hetf}} \right) S_{msm} - \mu \gamma_{msm}^{msm}, \\ \frac{d\sigma_{hetf}^{msm}}{dt} = -a_{hetf}(1 - \varepsilon_{hetf}) \beta_M^F \left[\alpha_{hetf} \frac{\gamma_{msm}}{N_{msm}} + (1 - \alpha_{hetf}) \frac{\gamma_{hetm}}{N_{hetm}} \right] S_{hetf} \\ \quad - a_{hetf}(1 - \varepsilon_{hetf}) \beta_M^F \left[\alpha_{hetf} \frac{I_{msm}}{N_{msm}} + (1 - \alpha_{hetf}) \frac{S_{hetm}}{N_{hetm}} \right] \sigma_{hetf}^{msm} - \mu \sigma_{hetf}^{msm}, \\ \frac{d\gamma_{hetf}^{msm}}{dt} = a_{hetf}(1 - \varepsilon_{hetf}) \beta_M^F \left[\alpha_{hetf} \frac{\gamma_{msm}}{N_{msm}} + (1 - \alpha_{hetf}) \frac{\gamma_{hetm}}{N_{hetm}} \right] S_{hetf} \\ \quad + a_{hetf}(1 - \varepsilon_{hetf}) \beta_M^F \left[\alpha_{hetf} \frac{I_{msm}}{N_{msm}} + (1 - \alpha_{hetf}) \frac{S_{hetm}}{N_{hetm}} \right] \sigma_{hetf}^{msm} - \mu \gamma_{hetf}^{msm}, \\ \frac{d\sigma_{hetm}^{msm}}{dt} = -a_{hetm}(1 - \varepsilon_{hetm}) \beta_F^M \left[\frac{\gamma_{hetf}^{msm}}{N_{hetf}} S_{hetm} + \frac{I_{hetf}}{N_{hetf}} \sigma_{hetm}^{msm} \right] - \mu \sigma_{hetm}^{msm}, \\ \frac{dS_{hetm}^{msm}}{dt} = a_{hetm}(1 - \varepsilon_{hetm}) \beta_F^M \left[\frac{\gamma_{hetf}^{msm}}{N_{hetf}} S_{hetm} + \frac{I_{hetf}}{N_{hetf}} \sigma_{hetm}^{msm} \right] - \mu \gamma_{hetm}^{msm}. \end{array} \right.$$

The equations (2.31), (2.32) can be written similarly, and are omitted for brevity. The only substantive difference between the systems is the presence of the terms in **bold** above; these terms do not contain any contribution from the spillover variable, and are only present in the equations in which the perturbed ε_j appears.

2.3 Simulation study: U.S. state of Georgia

In this section, we present the results for a simulation study of HIV transmission in the U.S. state of Georgia.

2.3.1 Model parameterization, initial conditions, and validation

The values for each parameter are provided in Table 3, and the initial conditions are given in Table 4. The initial population sizes were obtained using U.S. Census data [46]. We considered populations in the 18-65 age range, giving a total simulated population of 6,630,671 persons. Data from the Williams Institute indicated that 4.5% of the population over 18 identified as LGBT, and with 6% of LGBT persons over 65 [47]. These data further showed that 57% of those identifying as LGBT were female, with 20.3% identifying as Lesbian. From these calculations, we obtained estimates for the overall MSM, HETF, and HETM populations [47]. Values for HIV prevalence by group were obtained from NCHHSTP ATLAS [2]; subtracting these populations from the total population gave the initial susceptible population.

In Fig. 2.2, we depict the model outputs at baseline (using the values in Table 2) plotting prevalence on the left and annual incidence on the right. We observe good agreement with surveillance data for recent years for annual HIV infections (2017-19 for group specific figures; overall incidence is available additionally for 2020-22) and HIV prevalence (estimated diagnosed and undiagnosed 2017-19). Note that, due to distortions related to the COVID-19 pandemic, incidence estimates for the years 2020-22 are subject to considerable uncertainty [37, 38, 48, 2].

Parameter	Value	Source
$\Pi_{msm,hetf,hetm}$	3874, 65497, 63549 persons <i>per year</i>	Proportional, based on current population composition and growth rate of 0.5% [46]
$a_{msm,hetf,hetm}$	94.7, 47.3, 48.5 <i>per year</i>	[37, 23, 36]
$\delta_{msm,hetf,hetm}$	1/200, 1/100, 1/50 <i>per year</i>	[2]
$\varepsilon_{msm,hetf,hetm}$	0.089, 0.0003, 0 (dimensionless, cor- resp. 11000, 1000, 0 people, resp.)	[2]
μ	1/50 <i>per year</i>	Assumed
β_M^M	0.0008 (dimensionless)	[37, 23, 36]
β_F^M	0.0003 (dimensionless)	[37, 23, 36]
β_M^F	0.0004 (dimensionless)	[37, 23, 36]
$\bar{\eta}_{msm}$	0.858 (dimensionless)	[37, 23, 36]; prior used in (2.33) to compute time-varying η_{msm} using [25]
$\bar{\alpha}_{hetf}$	0.02 (dimensionless)	[37, 23, 36]; prior used in (2.33) to compute time-varying α_{hetf} using [25]

Table 3: Parameter values.

State variable	Value	Source
S_{msm}^0	123,418	[46, 47]
I_{msm}^0	42,000	[2]
S_{hetf}^0	3,260,101	[46, 47]
I_{hetf}^0	14,700	[2]
S_{hetm}^0	3,138,939	[46, 47]
I_{hetm}^0	7,000	[2]

Table 4: Basic model (2.1), Georgia simulation study: Initial conditions.

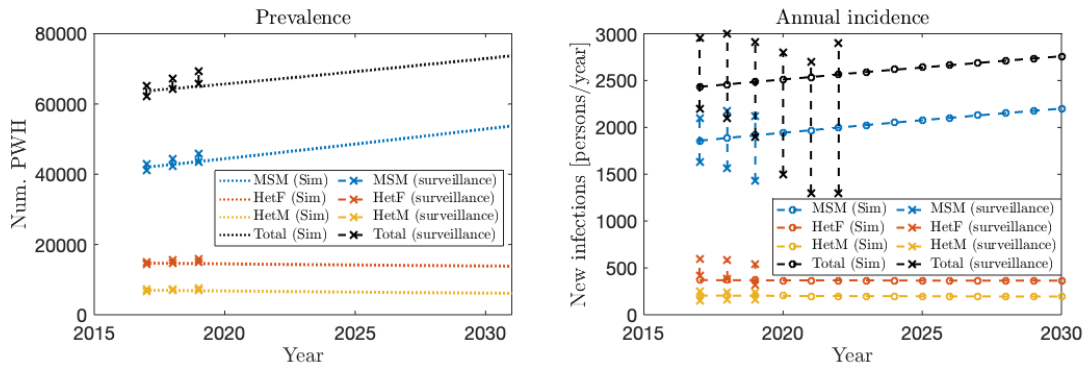


Figure 2.2: Basic model (2.1), Georgia simulation study: Baseline simulation and comparison against HIV surveillance data.

At each time step, we employ the algorithm introduced in [25] to ensure that the closure conditions (2.2) are satisfied. In practice, we define priors $\bar{\eta}_{msm}$, $\bar{\alpha}_{hetf}$, as inputs to the algorithm in [25], which then solve:

$$\arg \min_{\eta_{msm}, \alpha_{hetf}} (\eta_{msm} - \bar{\eta}_{msm})^2 + (\alpha_{hetf} - \bar{\alpha}_{hetf})^2, \quad \text{subject to (2.2)}. \quad (2.33)$$

2.3.2 Simulation and results

We consider nine intervention simulations, in which PrEP is administered to 10,000, 25,000, and 50,000 additional persons in the MSM, HETF, and HETM populations respectively. Our primary outcome of interest is total HIV incidence from 2020-30. Using our baseline simulation as a reference, we compute, for each simulation and each transmission group, the overall number of new HIV infections prevented as a result of the PrEP intervention.

We then solve the spillover equations (2.30), (2.31), and (2.32) (at baseline) applying the algorithm in [25] at each time step to ensure contact symmetry, and examine the effect on HIV incidence for each group resulting from delivery of PrEP to a given group.

The 10-year cumulative incidence and infections prevented for the whole population, as well as each transmission group, are given for each intervention scenario in Table 5. The results demonstrate that by far the largest reductions in incidence result from focusing PrEP delivery on MSM. Notably, on a per-person basis, delivering PrEP to MSM appears to be more effective in reducing incidence among HETF than giving PrEP to HETF directly.

This is further confirmed in Fig. 2.3, where we plot the direct and spillover effects γ_i^j of PrEP delivery, in terms of infections averted for each additional person on PrEP. As the plot on the left shows, there is no evidence of spillover onto the MSM population when PrEP is given to HETF or HETM. For HETF (Fig. 2.3 center), we see that the direct effect of giving PrEP to HETF is almost immediately overtaken by the spillover from PrEP delivery to MSM. Furthermore, while the direct effect of giving PrEP to HETF results in linear-in-time incidence reductions, PrEP delivery to MSM shows a nonlinear effect on incidence reduction, with an increasing rate of growth. By the end the time interval, the spillover effect on HETF from MSM is over five times larger than the effect of giving PrEP to HETF directly. For HETM, over the considered time interval, the largest incidence reductions come from direct delivery of PrEP to HETM. However, as with HETF, a significant spillover effect from MSM is nonetheless apparent, and shows an increasing rate of growth. It appears that, within a few more years, the spillover effect on incidence from PrEP delivery to MSM will overtake direct PrEP delivery to HETM in importance.

The related NNTs, see (2.14), are shown in Fig. 2.4. For MSM, the NNTs at the end of the simulation period are approximately 45 to prevent an infection among MSM, 2000 to prevent an infection among HETF, and 17000 to prevent an infection among HETM. For HETF, the NNT to prevent an infection among HETF is approximately 9000, and over 50,000 to prevent an infection among HETM by the end of the time period. As no infections were prevented among MSM due to increased PrEP delivery to HETF, the NNT is undefined in this case. Finally, the NNT for HETM was approximately 12500 to prevent an infection among HETM, and 30000 to prevent an infection among HETF (not pictured). We observe that NNTs decrease over longer time intervals, reflecting downstream effects of infection prevention. The NNT numbers for MSM are in line with [19, 49]; for heterosexuals, direct comparison is difficult due to ambiguity in the definition of underlying HIV transmission rate [19].

Overall, the results for the basic model (2.1) suggest that maximum incidence reductions are achieved when delivering PrEP to MSM. Due to the substantial spillover effects, PrEP delivery among MSM is a more efficient means of reducing incidence among HETF almost immediately. Furthermore, PrEP delivery to MSM results in significant reductions in incidence among HETM. Over long time horizons, delivering PrEP to MSM and exploiting the subsequent spillover effect appears to be the most effective means of incidence reduction among HETM as well, despite the lack of direct interaction between the groups.

3 Extended model with heterosexual female population stratified by risk factors

The model (2.1) assumes that all MSM, HETF, and HETM behave uniformly. In reality, however, behavior may differ substantially within these groups, resulting in subgroups with different risk and transmission profiles. For example, certain sub-populations within HETF have significantly elevated risk of HIV infection compared to the overall HETF population. Consequently, one may expect that PrEP interventions which successfully prioritize these higher-risk individuals may be more effective in preventing HIV infection. In fact, CDC PrEP eligibility guidelines are offered to help aid potential patients and medical professionals in identifying persons with elevated HIV risk [11, 19, 17].

To evaluate how prioritizing PrEP use among certain populations with more risk factors may change the overall effectiveness of PrEP interventions, we extend the model (2.1) by stratifying the heterosexual female population into

Scenario	10-yr total incidence (inf. prevented)	10-yr MSM incidence (inf. prevented)	10-yr HETF inci- dence (inf. prevented)	10-yr HETM inci- dence (inf. prevented)
Baseline	29,019	22,824	4,021	2,174
PrEP to 10,000 addi- tional MSM	26,613 (2,406)	20,478 (2,346)	3,963 (58)	2,172 (2)
PrEP to 25,000 addi- tional MSM	23,200 (5,819)	17,151 (5,673)	3,882 (139)	2,167 (7)
PrEP to 50,000 addi- tional MSM	18,026 (10,993)	12,094 (10,730)	3,769 (252)	2,163 (11)
PrEP to 10,000 addi- tional HETF	29,005 (14)	22,824 (0)	4,007 (14)	2,174 (0)
PrEP to 25,000 addi- tional HETF	28,986 (33)	22,824 (0)	3,990 (31)	2,172 (2)
PrEP to 50,000 addi- tional HETF	28,951 (68)	22,824 (0)	3,957 (64)	2,170 (4)
PrEP to 10,000 addi- tional HETM	29,012 (7)	22,824 (0)	4,019 (2)	2,170 (5)
PrEP to 25,000 addi- tional HETM	28,999 (20)	22,824 (0)	4,019 (2)	2,156 (18)
PrEP to 50,000 addi- tional HETM	28,981 (38)	22,824 (0)	4,017 (4)	2,140 (34)

Table 5: Basic model (2.1), Georgia simulation study: 10-year incidence and infections prevented among each transmission group, resulting from varying levels of PrEP given to each transmission group.

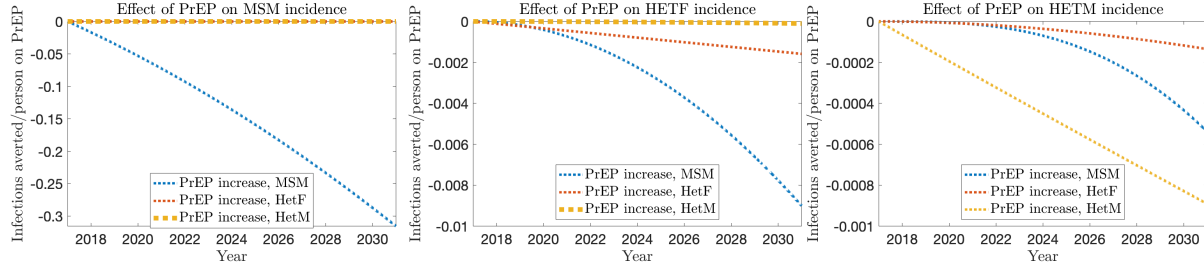


Figure 2.3: Basic model (2.1), Georgia simulation study: Effects on incidence among MSM, HETF, and HETM (left to right) as a result of administering PrEP to each group.

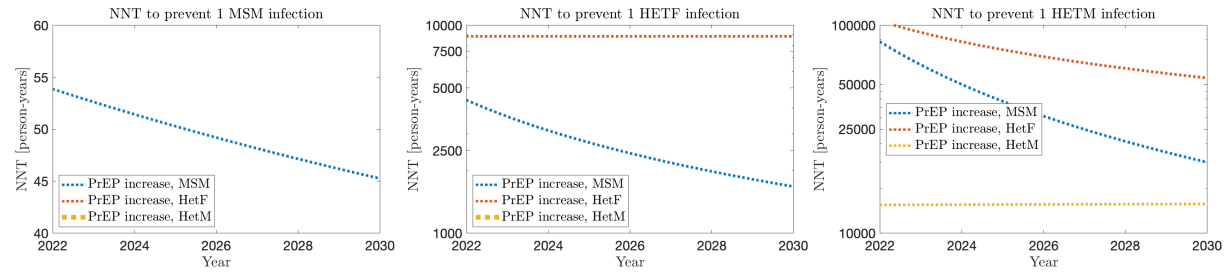


Figure 2.4: Basic model (2.1), Georgia simulation study: NNTs over the simulation period 2020-2030. Note that some curves are not displayed due to excessively high (or undefined) NNTs.

two subgroups: HETF with high risk factors $hetf_h$ and HETF with low risk factors $hetf_l$. We incorporate the two aforementioned subgroups in susceptible HETF population (which stratifies into high-risk susceptible HETF and low-risk infected HETF, denoted by S_{hetf_h} and S_{hetf_l} , respectively) and infected HETF population (which stratifies into high-risk infected HETF and low-risk infected HETF, denoted by I_{hetf_h} and I_{hetf_l} , respectively). Hence, the total number of individuals in each subgroup j at time t , is given by $N_j(t) = S_j(t) + I_j(t)$, (with $j = \{msm, hetf_h, hetf_l, hetm\}$).

State variable	Description
S_{msm}	Population of susceptible MSM
I_{msm}	Population of HIV-infected MSM
S_{hetf_h}	Population of susceptible high-risk HETF
I_{hetf_h}	Population of infected high-risk HETF
S_{hetf_l}	Population of susceptible low-risk HETF
I_{hetf_l}	Population of infected low-risk HETF
S_{hetm}	Population of susceptible HETM
S_{hetm}	Population of HIV-infected HETM

Table 6: Description of state variables of the risk-structured model (3.1).

Thus, the total population (in all subgroups) at time t , denoted by $N(t)$ is given by:

$$N(t) = N_{msm}(t) + N_{hetf_h}(t) + N_{hetf_l} + N_{hetm}(t).$$

The model follows the contact structure depicted in Fig. 3.1. The probabilities of HIV transmission per male to male contact, per female to male contact, and per male to female contact, are denoted by β_M^M , β_F^M , and β_F^F , respectively. The susceptible population increases with the recruitment of individuals into the sexually active population at rate Π_j , with $j = \{msm, hetf_h, hetf_l, hetm\}$. Further, HIV-infected individuals in each subgroup j die due to the disease at rate δ_j and natural death occurs in all sub-populations at a rate μ . Similarly to the basic model, it is assumed here that PrEP is administered to a fraction of sexually active susceptible individuals (i.e., ε_j) in each subgroup j . Thus, the extended model with heterosexual female population stratified by risk factors is given by the following system of equations:

$$\left\{ \begin{aligned} \frac{dS_{msm}}{dt} &= \Pi_{msm} - a_{msm}(1 - \varepsilon_{msm}) \left[\eta_{msm} \beta_M^M \frac{I_{msm}}{N_{msm}} + \eta_{hetf_h} \beta_F^M \frac{I_{hetf_h}}{N_{hetf_h}} \right. \\ &\quad \left. + (1 - \eta_{msm} - \eta_{hetf_h}) \beta_F^M \frac{I_{hetf_l}}{N_{hetf_l}} \right] S_{msm} - \mu S_{msm}, \\ \frac{dI_{msm}}{dt} &= a_{msm}(1 - \varepsilon_{msm}) \left[\eta_{msm} \beta_M^M \frac{I_{msm}}{N_{msm}} + \eta_{hetf_h} \beta_F^M \frac{I_{hetf_h}}{N_{hetf_h}} \right. \\ &\quad \left. + (1 - \eta_{msm} - \eta_{hetf_h}) \beta_F^M \frac{I_{hetf_l}}{N_{hetf_l}} \right] S_{msm} - (\mu + \delta_{msm}) I_{msm}, \\ \frac{dS_{hetf_h}}{dt} &= \Pi_{hetf_h} - a_{hetf_h}(1 - \varepsilon_{hetf_h}) \beta_F^M \left[\alpha_{hetf_h} \frac{I_{msm}}{N_{msm}} + (1 - \alpha_{hetf_h}) \frac{I_{hetm}}{N_{hetm}} \right] S_{hetf_h} - \mu S_{hetf_h}, \\ \frac{dI_{hetf_h}}{dt} &= a_{hetf_h}(1 - \varepsilon_{hetf_h}) \beta_F^M \left[\alpha_{hetf_h} \frac{I_{msm}}{N_{msm}} + (1 - \alpha_{hetf_h}) \frac{I_{hetm}}{N_{hetm}} \right] S_{hetf_h} - (\mu + \delta_{hetf_h}) I_{hetf_h}, \\ \frac{dS_{hetf_l}}{dt} &= \Pi_{hetf_l} - a_{hetf_l}(1 - \varepsilon_{hetf_l}) \beta_F^M \left[\alpha_{hetf_l} \frac{I_{msm}}{N_{msm}} + (1 - \alpha_{hetf_l}) \frac{I_{hetm}}{N_{hetm}} \right] S_{hetf_l} - \mu S_{hetf_l}, \\ \frac{dI_{hetf_l}}{dt} &= a_{hetf_l}(1 - \varepsilon_{hetf_l}) \beta_F^M \left[\alpha_{hetf_l} \frac{I_{msm}}{N_{msm}} + (1 - \alpha_{hetf_l}) \frac{I_{hetm}}{N_{hetm}} \right] S_{hetf_l} - (\mu + \delta_{hetf_l}) I_{hetf_l}, \\ \frac{dS_{hetm}}{dt} &= \Pi_{hetm} - a_{hetm}(1 - \varepsilon_{hetm}) \beta_F^M \left[\xi_{hetm} \frac{I_{hetf_h}}{N_{hetf_h}} + (1 - \xi_{hetm}) \frac{I_{hetf_l}}{N_{hetf_l}} \right] S_{hetm} - \mu S_{hetm}, \\ \frac{dI_{hetm}}{dt} &= a_{hetm}(1 - \varepsilon_{hetm}) \beta_F^M \left[\xi_{hetm} \frac{I_{hetf_h}}{N_{hetf_h}} + (1 - \xi_{hetm}) \frac{I_{hetf_l}}{N_{hetf_l}} \right] S_{hetm} - (\mu + \delta_{hetm}) I_{hetm}. \end{aligned} \right. \quad (3.1)$$

together with suitable initial conditions. The state variables and parameters are described in Tables 6 and 7, respectively. Additionally, the following closure conditions must be satisfied:

$$\begin{aligned} \eta_{hetf_h} N_{msm} a_{msm} &= \alpha_{hetf_h} N_{hetf_h} a_{hetf_h}, \\ (1 - \eta_{msm} - \eta_{hetf_h}) N_{msm} a_{msm} &= \alpha_{hetf_l} N_{hetf_l} a_{hetf_l}, \\ (1 - \alpha_{hetf_h}) N_{hetf_h} a_{hetf_h} &= \xi_{hetm} N_{hetm} a_{hetm}, \\ (1 - \alpha_{hetf_l}) N_{hetf_l} a_{hetf_l} &= (1 - \xi_{hetm}) N_{hetm} a_{hetm}. \end{aligned} \quad (3.2)$$

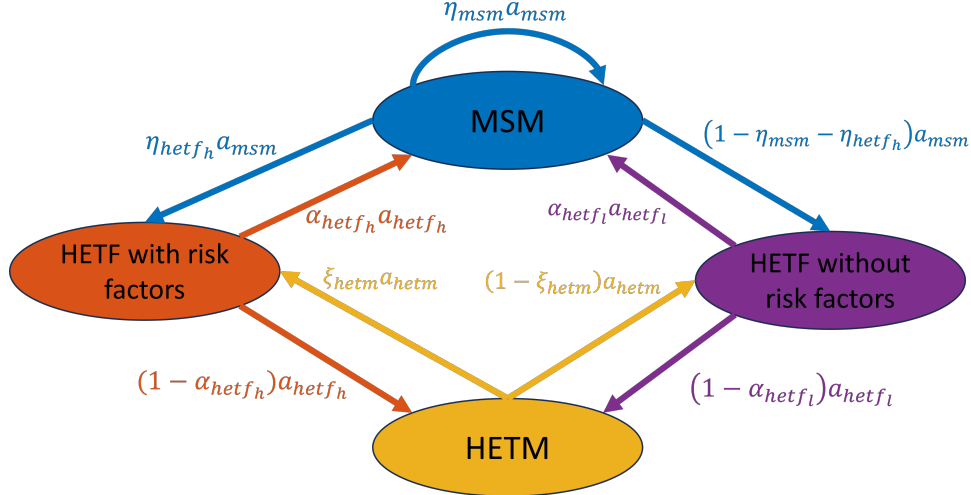


Figure 3.1: Sexual contact structure of the risk-structured model (3.1).

Parameter	Description
Π_j ($j = msm, hetf_h, hetf_l, hetm$)	Recruitment rate
a_j ($j = msm, hetf_h, hetf_l, hetm$)	Number of contacts <i>per year</i> for group j
δ_j ($j = msm, hetf_h, hetf_l, hetm$)	Disease-induced mortality for group j
ε_j ($j = msm, hetf_h, hetf_l, hetm$)	Fraction of group j on PrEP
μ	Natural death rate
β_M^M	Probability of HIV transmission per male-to-male contact
β_F^M	Probability of HIV transmission per female-to-male contact
β_M^F	Probability of HIV transmission per male-to-female contact
η_{msm}	Proportion of MSM contacts that are with MSM
η_{hetf_h}	Proportion of MSM contacts that are with high-risk HETF
α_{hetf_h}	Proportion of high-risk HETF contacts that are with MSM
α_{hetf_l}	Proportion of low-risk HETF contacts that are with MSM
ξ_{hetm}	Proportion of HETM contacts that are with high-risk HETF

Table 7: Description of parameters of the risk-structured model (3.1).

3.1 Mathematical analysis

Well-posedness, local and global stability can be rigorously established for the model (3.1) following arguments similar to those used for (2.1). The complete analysis is provided in Appendix C. Below, we provide a brief analysis of the local stability, intended to provide an intuitive, qualitative interpretation of the model behavior.

3.1.1 Local asymptotic stability of the disease-free equilibrium of the risk-structured model

The disease-free equilibrium \mathcal{E}_r of the risk-structured model (3.1) is given by:

$$\mathcal{E}_r = (S_{msm}^{**}, I_{msm}^{**}, S_{hetf_h}^{**}, I_{hetf_h}^{**}, S_{hetf_l}^{**}, I_{hetf_l}^{**}, S_{hetm}^{**}, I_{hetm}^{**}) = \left(\frac{\Pi_{msm}}{\mu}, 0, \frac{\Pi_{hetf_h}}{\mu}, 0, \frac{\Pi_{hetf_l}}{\mu}, 0, \frac{\Pi_{hetm}}{\mu} \right). \quad (3.3)$$

Similarly to the analysis of (2.1), we use the next-generation method [44, 43] to analyze the local asymptotic stability of \mathcal{E}_r . Using the same notation as used in Section 2.1.1, the matrices F_r and V_r are given by:

$$F_r = \begin{bmatrix} f_{11_r} & f_{12_r} & f_{13_r} & 0 \\ f_{21_r} & 0 & 0 & f_{24_r} \\ f_{31_r} & 0 & 0 & f_{34_r} \\ 0 & f_{42_r} & f_{43_r} & 0 \end{bmatrix} \quad \text{and} \quad V_r = \begin{bmatrix} K_{1_r} & 0 & 0 & 0 \\ 0 & K_{2_r} & 0 & 0 \\ 0 & 0 & K_{3_r} & 0 \\ 0 & 0 & 0 & K_{4_r} \end{bmatrix}, \quad (3.4)$$

where (noting that $N_{msm}^{**} = S_{msm}^{**}$, $N_{hetfh}^{**} = S_{hetfh}^{**}$, $N_{hetfi}^{**} = S_{hetfi}^{**}$, $N_{hetm}^{**} = S_{hetm}^{**}$)

$$\begin{aligned} f_{11_r} &= \frac{[a_{msm}(1 - \varepsilon_{msm})\eta_{msm}\beta_M^M] S_{msm}^{**}}{N_{msm}^{**}}, & f_{12_r} &= \frac{[a_{msm}(1 - \varepsilon_{msm})\eta_{hetfh}\beta_F^M] S_{msm}^{**}}{N_{hetfh}^{**}}, \\ f_{13_r} &= \frac{[a_{msm}(1 - \varepsilon_{msm})(1 - \eta_{msm} - \eta_{hetfh})\beta_F^M] S_{msm}^{**}}{N_{hetfi}^{**}}, \\ f_{21_r} &= \frac{[a_{hetfh}(1 - \varepsilon_{hetfh})\alpha_{hetfh}\beta_M^F] S_{hetfh}^{**}}{N_{msm}^{**}}, & f_{24_r} &= \frac{[a_{hetfh}(1 - \varepsilon_{hetfh})(1 - \alpha_{hetfh})\beta_M^F] S_{hetfh}^{**}}{N_{hetm}^{**}}, \\ f_{31_r} &= \frac{[a_{hetfi}(1 - \varepsilon_{hetfi})\alpha_{hetfi}\beta_M^F] S_{hetfi}^{**}}{N_{msm}^{**}}, & f_{34_r} &= \frac{[a_{hetfi}(1 - \varepsilon_{hetfi})(1 - \alpha_{hetfi})\beta_M^F] S_{hetfi}^{**}}{N_{hetm}^{**}}, \\ f_{42_r} &= \frac{[a_{hetm}(1 - \varepsilon_{hetm})\xi_{hetm}\beta_F^M] S_{hetm}^{**}}{N_{hetfh}^{**}}, & f_{43_r} &= \frac{[a_{hetm}(1 - \varepsilon_{hetm})(1 - \xi_{hetm})\beta_F^M] S_{hetm}^{**}}{N_{hetfi}^{**}}. \end{aligned}$$

Furthermore, we have that

$$K_{1_r} = \mu + \delta_{msm}, \quad K_{2_r} = \mu + \delta_{hetfh}, \quad K_{3_r} = \mu + \delta_{hetfi}, \quad K_{4_r} = \mu + \delta_{hetm}.$$

Here too, it is also convenient to define the quantity (where ρ is the spectral radius) [43]:

$$\mathbb{R}_{cr} = \rho(F_r V_r^{-1}) = \max\{\mathbb{R}_{cr1}, \mathbb{R}_{cr2}, \mathbb{R}_{cr3}, \mathbb{R}_{cr4}\},$$

where

$$\mathbb{R}_{cr1} = \frac{f_{11}}{4K_{1_r}} - H_1 - H_3, \quad \mathbb{R}_{cr2} = \frac{f_{11}}{4K_{1_r}} + H_1 - H_3, \quad \mathbb{R}_{cr3} = \frac{f_{11}}{4K_{1_r}} + H_3 - H_2, \quad \text{and} \quad \mathbb{R}_{cr4} = \frac{f_{11}}{4K_{1_r}} + H_2 + H_3.$$

The complete definitions of H_1 , H_2 , and H_3 are complex and can be found in Appendix C; they define the interaction of transmission across the population groups (analogously to the terms $G_{1,2,3,4}$ in the analysis of (2.1)). However, we note that the term $f_{11}/4K_{1_r}$, which depends only on MSM-related transmission quantities, appears in each term $\mathbb{R}_{cr1, cr2, cr3, cr4}$. Qualitatively, this shows that a significant component of HIV transmission depends on MSM-dynamics, independently of other populations; therefore if $f_{11}/4K_{1_r} \gg 1$, then it is possible for $\mathbb{R}_{cr} > 1$, regardless of transmission levels in other groups.

3.2 Qualitative analysis and assessment of PrEP spillover effects: risk-structured model

The derivation of the spillover equations for the model (3.1), again for the case of $\delta_j = 0$, $j = msm, hetfh, hetfi, hetm$, follows a procedure analogous to the one shown for the model (2.1) in Section 2.2.1. Hence, we do not repeat the arguments shown in that section for brevity and to avoid redundancy. We employ an analogous notation as before, slightly modifying (2.20) as follows to account for the additional stratification:

$$\begin{aligned} \mathbf{X} &= \begin{pmatrix} S_{msm} \\ I_{msm} \\ S_{hetfh} \\ I_{hetfh} \\ S_{hetfi} \\ I_{hetfi} \\ S_{hetm} \\ I_{hetm} \end{pmatrix}, \quad \mathbf{\Lambda}_{msm} = \begin{pmatrix} 0 \\ a_{msm}\eta_{msm}\frac{\beta_M^M}{N_{msm}} \\ 0 \\ a_{msm}\eta_{hetfh}\frac{\beta_F^M}{N_{hetfh}} \\ 0 \\ a_{msm}(1 - \eta_{msm} - \eta_{hetfh})\frac{\beta_F^M}{N_{hetfi}} \\ 0 \\ 0 \end{pmatrix}, \quad \mathbf{\Lambda}_{hetfh} = \begin{pmatrix} 0 \\ a_{hetfh}\alpha_{hetfh}\frac{\beta_M^F}{N_{msm}} \\ 0 \\ 0 \\ 0 \\ 0 \\ 0 \\ a_{hetfh}(1 - \alpha_{hetfh})\frac{\beta_F^M}{N_{hetm}} \end{pmatrix}, \\ \mathbf{\Lambda}_{hetfi} &= \begin{pmatrix} 0 \\ a_{hetfi}\alpha_{hetfi}\frac{\beta_M^F}{N_{msm}} \\ 0 \\ 0 \\ 0 \\ 0 \\ 0 \\ a_{hetfi}(1 - \alpha_{hetfi})\frac{\beta_F^M}{N_{hetm}} \end{pmatrix}, \quad \mathbf{\Lambda}_{hetm} = \begin{pmatrix} 0 \\ 0 \\ 0 \\ a_{hetm}\gamma_h\frac{\beta_F^M}{N_{hetfh}} \\ 0 \\ a_{hetm}(1 - \gamma_h)\frac{\beta_F^M}{N_{hetfi}} \\ 0 \\ 0 \end{pmatrix}, \quad \mathbf{\vartheta}^{msm} = \begin{pmatrix} \sigma_{msm}^{msm} \\ \gamma_{msm}^{msm} \\ \sigma_{msm}^{msm} \\ \sigma_{hetfh}^{msm} \\ \gamma_{hetfh}^{msm} \\ \sigma_{hetfi}^{msm} \\ \gamma_{hetfi}^{msm} \\ \sigma_{hetm}^{msm} \\ \gamma_{hetm}^{msm} \end{pmatrix}. \end{aligned} \tag{3.5}$$

Then, the spillover equations describing the effect of giving PrEP to MSM in model (3.1) read:

$$\left\{ \begin{array}{lcl} \frac{d\sigma_{msm}^{msm}}{dt} & = & -(1 - \varepsilon_{msm}) [(\Lambda_{msm}^T \boldsymbol{\vartheta}^{msm}) S_{msm} + (\Lambda_{msm}^T \mathbf{X}) \sigma_{msm}^{msm}] + (\Lambda_{msm}^T \mathbf{X}) S_{msm} - \mu \sigma_{msm}^{msm}, \\ \frac{d\gamma_{msm}^{msm}}{dt} & = & (1 - \varepsilon_{msm}) [(\Lambda_{msm}^T \boldsymbol{\vartheta}^{msm}) S_{msm} + (\Lambda_{msm}^T \mathbf{X}) \sigma_{msm}^{msm}] - (\Lambda_{msm}^T \mathbf{X}) S_{msm} - \mu \gamma_{msm}^{msm}, \\ \frac{d\sigma_{hetfh}^{msm}}{dt} & = & -(1 - \varepsilon_{hetfh}) [(\Lambda_{hetfh}^T \boldsymbol{\vartheta}^{msm}) S_{hetfh} + (\Lambda_{hetfh}^T \mathbf{X}) \sigma_{hetfh}^{msm}] - \mu \sigma_{hetfh}^{msm}, \\ \frac{d\gamma_{hetfh}^{msm}}{dt} & = & (1 - \varepsilon_{hetfh}) [(\Lambda_{hetfh}^T \boldsymbol{\vartheta}^{msm}) S_{hetfh} + (\Lambda_{hetfh}^T \mathbf{X}) \sigma_{hetfh}^{msm}] - \mu \gamma_{hetfh}^{msm}, \\ \frac{d\sigma_{hetfi}^{msm}}{dt} & = & -(1 - \varepsilon_{hetfi}) [(\Lambda_{hetfi}^T \boldsymbol{\vartheta}^{msm}) S_{hetfi} + (\Lambda_{hetfi}^T \mathbf{X}) \sigma_{hetfi}^{msm}] - \mu \sigma_{hetfi}^{msm}, \\ \frac{d\gamma_{hetfi}^{msm}}{dt} & = & (1 - \varepsilon_{hetfi}) [(\Lambda_{hetfi}^T \boldsymbol{\vartheta}^{msm}) S_{hetfi} + (\Lambda_{hetfi}^T \mathbf{X}) \sigma_{hetfi}^{msm}] - \mu \gamma_{hetfi}^{msm}, \\ \frac{d\sigma_{hetm}^{msm}}{dt} & = & -(1 - \varepsilon_{hetm}) [(\Lambda_{hetm}^T \boldsymbol{\vartheta}^{msm}) S_{hetm} + (\Lambda_{hetm}^T \mathbf{X}) \sigma_{hetm}^{msm}] - \mu \sigma_{hetm}^{msm}, \\ \frac{d\gamma_{hetm}^{msm}}{dt} & = & (1 - \varepsilon_{hetm}) [(\Lambda_{hetm}^T \boldsymbol{\vartheta}^{msm}) S_{hetm} + (\Lambda_{hetm}^T \mathbf{X}) \sigma_{hetm}^{msm}] - \mu \gamma_{hetm}^{msm}. \end{array} \right.$$

As in the basic model, the initial conditions are homogeneously zero in each compartment. The corresponding equations for giving the spillover effect in terms of *number* of persons on PrEP can be obtained following the same reasoning as in (2.11). Additionally, one can calculate the effect of PrEP on *incidence* (only new infections) analogously as in (2.12) as well as approximate the NNT analogously to (2.14).

3.3 Simulation study: U.S. state of Georgia

As was done for (2.1), we now perform an analogous set of simulations for (3.1).

3.3.1 Model parameterization, initial conditions, and validation

The values of the model parameters and initial conditions are given in Tables 8 and 9, respectively.

The parameters and initial conditions are largely identical to those used in the three-population case (see Tables 3, 4). To ensure the conditions (3.2) are satisfied, we proceed as in the three-population case, and define priors $\bar{\eta}_{msm}$, $\bar{\eta}_{hetfh}$, $\bar{\alpha}_{hetfh}$, $\bar{\alpha}_{hetfi}$, $\bar{\xi}_{hetm}$, as inputs to the algorithm in [25], which then solve:

$$\arg \min_{\eta_{msm}, \eta_{hetfh}, \alpha_{hetfh}, \alpha_{hetfi}, \xi_{hetm}} f(\eta_{msm}, \eta_{hetfh}, \alpha_{hetfh}, \alpha_{hetfi}, \xi_{hetm}) \quad \text{subject to (3.2),} \quad (3.6)$$

with,

$$f = (\eta_{msm} - \bar{\eta}_{msm})^2 + (\eta_{hetfh} - \bar{\eta}_{hetfh})^2 + (\alpha_{hetfh} - \bar{\alpha}_{hetfh})^2 + (\alpha_{hetfi} - \bar{\alpha}_{hetfi})^2 + (\xi_{hetm} - \bar{\xi}_{hetm})^2.$$

We show the comparison of the baseline model scenario with surveillance data in Fig. 3.2. We observe that simulated incidence and prevalence are in good agreement with surveillance data. The baseline behavior of (2.1) and (3.1) is similar, both qualitatively and quantitatively.

3.3.2 Simulation and results

The simulation setup is analogous to the three-population simulations. We consider twelve total interventions, in which PrEP is administered to 10,000, 25,000, and 50,000 additional persons in the MSM, high-risk HETF, low-risk HETF and HETM populations respectively. The intervention begins in model year 2020 and our primary outcome of interest is total HIV incidence from 2020-30. As was done previously, we take our baseline simulation as a reference, we compute, for each simulation and each transmission group, the overall number of new HIV infections prevented as a result of the PrEP intervention.

We then solve the spillover equations derived in Section 3.2 (at baseline levels of PrEP), and examine the direct effect on HIV incidence for each group resulting from delivery of PrEP to a given group, and on the NNTs.

The 10-year incidence, both overall and for each transmission group, are reported for each simulated scenario in Table 10. The results at baseline, and for the HETM- and MSM-focused interventions, are very similar to the three-population

Parameter	Value	Source
$\Pi_{msm,hetf_h,hetf_l,hetm}$	3784, 3275, 62222, 63549 persons <i>per year</i>	Proportional, based on current population composition and growth rate of 0.5% [46]
$a_{msm,hetf_h,hetf_l,hetm}$	94.7, 91, 43.7, 48.5 <i>per year</i>	[37, 23, 36]
$\delta_{msm,hetf_h,hetf_l,hetm}$	1/200, 1/50, 1/100, 1/50 <i>per year</i>	[2]
$\varepsilon_{msm,hetf_h,hetf_l,hetm}$	0.089, 0.0061, 0, 0 (dimensionless, corresp. 11000, 1000, 0, 0 people, resp.). (dimensionless)	[2]
μ	1/50 <i>per year</i>	Assumed
β_M^M	0.0008 (dimensionless)	[37, 23, 36]
β_F^M	0.0003 (dimensionless)	[37, 23, 36]
β_M^F	0.0004 (dimensionless)	[37, 23, 36]
$\bar{\eta}_{msm,hetf_h}$	0.858, 0.071 (dimensionless)	[37, 23, 36]; priors used in (3.6) to compute time-varying $\eta_{msm,hetf_h}$ using [25]
$\bar{\alpha}_{hetf_h}$	0.06 (dimensionless)	[37, 23, 36]; prior used in (3.6) to compute time-varying α_{hetf_h} using [25]
$\bar{\alpha}_{hetf_l}$	0.01 (dimensionless)	[37, 23, 36]; prior used in (3.6) to compute time-varying α_{hetf_l} using [25]
$\bar{\xi}_{hetm}$	0.005 (dimensionless)	[37, 23, 36]; prior used in (3.6) to compute time-varying ξ_{hetfm} using [25]

Table 8: Risk-structured model (3.1), Georgia simulation study: Parameter values.

State variable	Value	Source
S_{msm}^0	123,418	[46, 47]
I_{msm}^0	42,000	[2]
$S_{hetf_h}^0$	243,340	[46, 47], 7.7% of HETF population [37, 36]
$I_{hetf_h}^0$	8,820	[2, 47], 60% of PWH among HETF [37, 36]
S_{lh}^0	3,016,762	[46, 47], 92.3% of HETF population [37, 36]
I_{lh}^0	5,880	[2, 47], 40% of PWH among HETF [37, 36]
S_{hetm}^0	3,138,939	[46, 47]
I_{hetm}^0	7,000	[2]

Table 9: Risk-structured model (3.1), Georgia simulation study: Initial conditions.

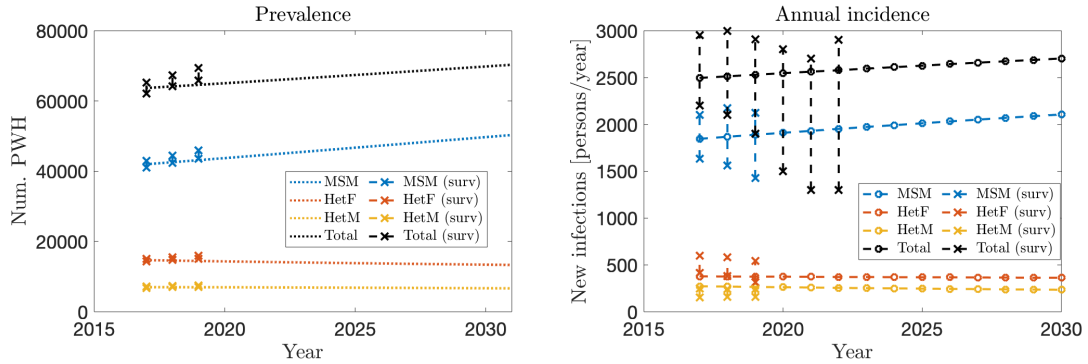


Figure 3.2: Risk-structured model (3.1), Georgia simulation study: Baseline simulation and comparison against HIV surveillance data.

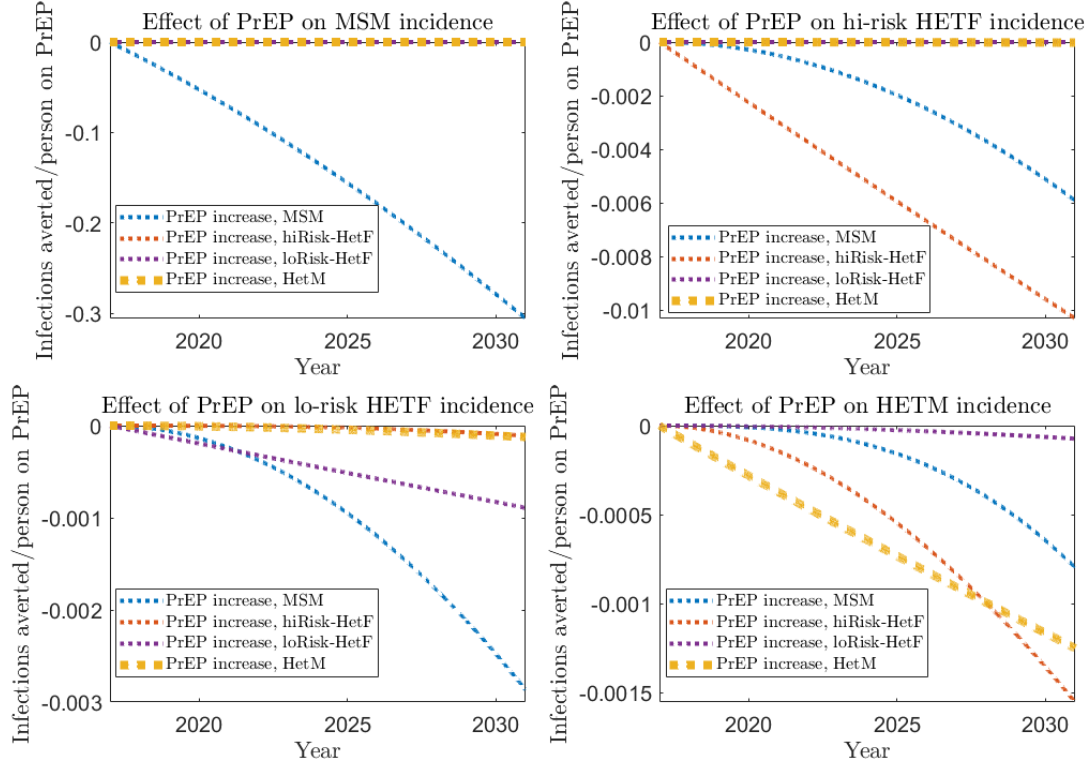


Figure 3.3: Risk-structured model (3.1), Georgia simulation study: Effects on incidence among MSM, High-risk HETF, Low-risk HETF, and HETM (clockwise, from top-left) as a result of administering PrEP to each group.

results. In particular, we see that giving PrEP to HETM results in minimal spillover to other groups, and that giving PrEP to MSM results in notable spillover to HETF, and modest spillover to HETM.

However, we observe notable qualitative and quantitative differences in the effects of PrEP interventions on the HETF populations. When PrEP is delivered to high-risk HETF, we observe a significant reduction in incidence among HETF. In this case, the direct effect of giving PrEP to high-risk HETF is larger than the corresponding spillover effect resulting from delivering PrEP to MSM. This contrasts with the three-population model, in which spillover from MSM provided larger incidence reductions among HETF than direct PrEP delivery to HETF. Additionally, we see that, when PrEP is delivered to high-risk HETF, the spillover effect on HIV incidence among HETM is larger than the effect of giving PrEP to HETM directly.

On the other hand, when looking at the effects of PrEP delivery to low-risk HETF, the situation is very different. PrEP delivery to the low-risk HETF group results in very small reductions in HETF incidence. For this population, it appears that the spillover effect of PrEP delivery to MSM remains the most efficient means of incidence reduction. Notably, while delivery of PrEP to high-risk HETF had a significant spillover effect on HETM, delivery of PrEP to low-risk HETF did not prevent a single HETM infection over the 10-year period.

We plot the calculated spillover effects in Fig. 3.3, and the corresponding NNTs in Fig. 3.4. Among high-risk HETF, while we do observe spillover from MSM, it is not nearly as large as the direct effect of PrEP delivery to high-risk HETF. Conversely, for low-risk HETF, the dynamics are more similar to those seen in the three-population model, and the spillover effect from MSM overtakes the direct effect relatively quickly, and grows at an increasing rate. For HETM, the spillover effect from high-risk HETF overtakes the direct effect after a few years, and also grows at an increasing rate in time. Furthermore, we once again see a significant spillover effect from MSM on HETM, and it does appear that this will eventually be larger than the direct effect of giving PrEP to HETM over a longer time horizon. As in the three-population model, no group exhibited a significant spillover effect on MSM.

Scenario	10-yr total incidence (inf. prevented)	10-yr MSM incidence (inf. prevented)	10-yr HETF inci- dence (inf. prevented)	10-yr HETM inci- dence (inf. prevented)
Baseline	29,644	22,783	4,132	2,729
PrEP to 10,000 addi- tional MSM	27,242 (2,402)	20,441 (2,342)	4,076 (56)	2,725 (4)
PrEP to 25,000 addi- tional MSM	23,838 (5,806)	17,122 (5,661)	3,998 (134)	2,718 (11)
PrEP to 50,000 addi- tional MSM	18,667 (10,977)	12,078 (10,705)	3,879 (253)	2,710 (19)
PrEP to 10,000 addi- tional Hi-risk HETF	29,548 (96)	22,782 (1)	4,047 (85)	2,719 (10)
PrEP to 25,000 addi- tional Hi-risk HETF	29,405 (239)	22,781 (2)	3,922 (210)	2,702 (27)
PrEP to 50,000 addi- tional Hi-risk HETF	29,163 (481)	22,777 (6)	3,711 (421)	2,675 (54)
PrEP to 10,000 addi- tional Lo-risk HETF	29,636 (8)	22,783 (0)	4,124 (8)	2,729 (0)
PrEP to 25,000 addi- tional Lo-risk HETF	29,627 (17)	22,783 (0)	4,115 (17)	2,729 (0)
PrEP to 50,000 addi- tional Lo-risk HETF	29,608 (36)	22,783 (0)	4,096 (36)	2,729 (0)
PrEP to 10,000 addi- tional HETM	29,631 (13)	22,783 (0)	4,130 (2)	2,718 (11)
PrEP to 25,000 addi- tional HETM	29,618 (26)	22,783 (0)	4,129 (3)	2,706 (23)
PrEP to 50,000 addi- tional HETM	29,591 (53)	22,783 (0)	4,127 (5)	2,681 (48)

Table 10: Risk-structured model (3.1), Georgia simulation study: 10-year incidence and infections prevented among each transmission group, resulting from varying levels of PrEP given to each transmission group.

4 A large-scale model: the HOPE model

In this section we consider a large-scale HIV transmission model, the HOPE model (see [38, 37, 23, 36] and the associated technical reports). This is a realistic, national-level model, which considers populations stratified by age, race/ethnicity, transmission group, sex assigned at birth, HIV disease stage and care status. The HOPE model also considers HIV transmission due to persons who inject drugs (PWID), approximately 7% of annual transmissions in the US in recent years [2], who were not considered in the two simplified models (2.1) and (3.1). In total, HOPE considers 273 different populations, and nearly 3,000 individual parameters. Therefore, direct derivation of spillover equations, as was performed for the simpler models (2.1), (3.1), is neither practical nor feasible.

Numerical approaches are thus required for studying spillover effects. In the present work, we propose to use a sensitivity analysis technique, the so-called *Sobol decomposition method* [50] to measure the influence of input uncertain parameters on the model outcomes of interest. We thus slightly change perspective with respect to the previous sections: the model outcomes are considered to be uncertain, with the uncertainty being the result of the propagation of the uncertainty affecting the input parameters. Such uncertainty is included in the model by assuming that the input parameters are modeled by random variables. The Sobol method is then based on a decomposition of the variance of the output and returns some indicators, the so-called *Sobol indices*, that quantify the contribution of each input parameter to such variance. We consider two sets of them: the *first-order Sobol indices* measure the individual contribution of each parameter to the output variance, the *total Sobol indices* instead quantify the contributions of each parameter combined with the others. In the following we are mostly interested in the latter, as they allow to explore the joint influence of PrEP delivery to different transmission groups.

Specifically, to study the spillover effects for the HOPE model, we focus on the sensitivity of the HIV incidence in the four transmission groups MSM, HETF, HETM, and PWID to PrEP delivery in each of them. Note that, as hinted above, the HOPE model also considers other population stratifications (e.g. age and race/ethnicity, reaching 273 population groups); as such, for the purpose of this analysis we consider aggregations of all MSM populations, all

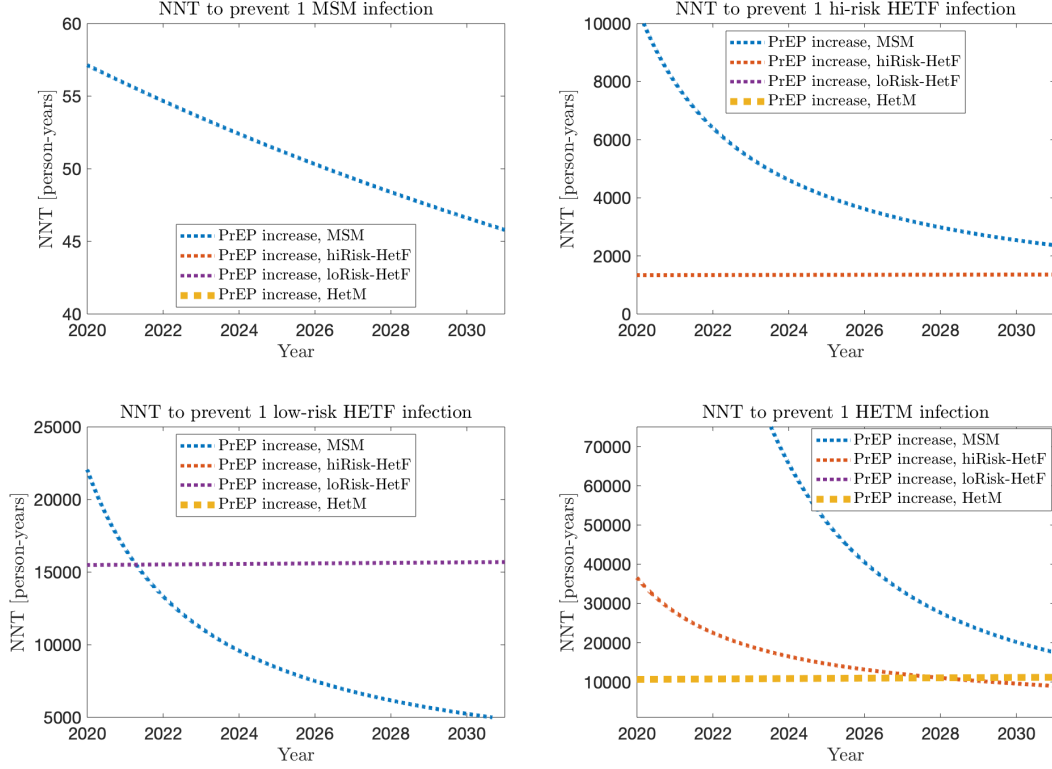


Figure 3.4: Risk-structured model (3.1), Georgia simulation study: NNTs over the simulation period 2020-2030. Note that some curves not visible due to excessively high NNTs.

HETF populations, etc. Thus, let us denote by \mathcal{I}_j a set of indices i_j denoting populations subgroups for each of the macro transmission group $j \in \{\text{MSM}, \text{HETF}, \text{HETM}, \text{PWID}\}$. We assume the fraction of individuals in each subgroup who are on PrEP, denoted by ε_{i_j} , to be modeled as follows

$$\varepsilon_{i_j} = \varepsilon_{i_j}^0 (1 + \theta_j), \quad i_j \in \mathcal{I}_j, \quad j = \{\text{MSM}, \text{HETF}, \text{HETM}, \text{PWID}\}, \quad (4.1)$$

where $\varepsilon_{i_j}^0$ is the level of PrEP coverage in group i_j at baseline and θ_j is a random parameter. We assume θ_j , $j \in \{\text{MSM}, \text{HETF}, \text{HETM}, \text{PWID}\}$ to be independent and uniformly distributed, taking values in the interval $\Gamma_j \subset \mathbb{R}$, with $\rho_j(\theta_j) : \Gamma_j \rightarrow [0, \infty)$ being the corresponding probability density functions (pdf). Then the corresponding random vector $\boldsymbol{\theta} = [\theta_{msm}, \theta_{hetf}, \theta_{hetm}, \theta_{pwid}]$ takes values in $\Gamma = \Gamma_{msm} \times \Gamma_{hetf} \times \Gamma_{hetm} \times \Gamma_{pwid} \subset \mathbb{R}^4$ and its joint pdf is given by:

$$\rho(\boldsymbol{\theta}) = \prod_{j \in \{\text{MSM}, \text{HETF}, \text{HETM}, \text{PWID}\}} \rho_j(\theta_j) \quad \forall \boldsymbol{\theta} \in \Gamma. \quad (4.2)$$

The reason we express variation in PrEP uptake as a relative change from baseline (cf. (4.1)) is practical: the HOPE model includes additional stratifications, however, our focus in the present is specifically on transmission group effects. To avoid overparameterization and maintain interpretability, we apply the same multiplicative adjustment θ_j across all subpopulations within each transmission group. For example, all MSM subgroups—regardless of age or race—receive the same proportional change in PrEP uptake.

We then denote by y a generic outcome of interest of the HOPE model such that

$$y : \Gamma \mapsto \mathbb{R}, \quad y(\boldsymbol{\theta}) = J(\mathbf{x}(t, \boldsymbol{\theta})), \quad (4.3)$$

where J is a bounded and continuous operator, possibly nonlinear, that acts on the model state $\mathbf{x} = \mathbf{x}(t, \boldsymbol{\theta}) \in \mathbb{R}^n$, with $n = 273$. In the context of the present work, y represents the annual HIV incidence among MSM, HETF, HETM, and

PWID macro populations. Hence, the incidence (recalling (2.8)) in the j -th group is then defined as:

$$\lambda_j(t, \boldsymbol{\theta}) = \sum_{i_j=1}^{|\lambda_j|} \lambda_{i_j}(t, \boldsymbol{\theta})$$

and the annual incidence $I_j^{year}(\boldsymbol{\theta})$ is obtained summing up the incidence $\lambda_j(t, \boldsymbol{\theta})$ over the year, i.e.

$$\lambda_j^{year}(\boldsymbol{\theta}) = \int_{t \in \text{year}} \lambda_j(t, \boldsymbol{\theta}) dt. \quad (4.4)$$

4.1 Sobol sensitivity indices

The goal of this section is to briefly illustrate the basics of the computation of Sobol indices. In this work we resort to the methodology based on the so-called generalized Polynomial Chaos Expansion (gPCE) (see e.g. [51, 52, 53]) that represents the random model outcome as a polynomial series, where the polynomials retain the uncertainty and the coefficients are deterministic. Then, the Sobol indices [39] can be computed by algebraic manipulations of those coefficients. For an overview on other options we refer to e.g. [54, 55, 40].

Let us introduce a generic set $\mathcal{M} \in \mathbb{N}^4$ of multi-indices $\mathbf{p} = [p_1, p_2, p_3, p_4]$. Let $\mathcal{P}_{\mathbf{p}} = \prod_{k=1}^4 P_{p_k}(\theta_k)$ denote a multivariate polynomial, given by the product of univariate polynomials of degree p_k (note that $P_0 = 1$), that are ρ_k -orthonormal, i.e. it holds that

$$\int_{\Gamma} \mathcal{P}_{\mathbf{p}}(\boldsymbol{\theta}) \mathcal{P}_{\mathbf{q}}(\boldsymbol{\theta}) \rho(\boldsymbol{\theta}) d\boldsymbol{\theta} = \delta_{\mathbf{p}\mathbf{q}}, \quad (4.5)$$

where $\delta_{\mathbf{p}\mathbf{q}}$ denotes the Kronecker Delta. Then, the gPCE is an approximation \tilde{y} of y in (4.3) of the following form

$$\tilde{y}(\boldsymbol{\theta}) \approx \sum_{\mathbf{p} \in \mathcal{M}} d_{\mathbf{p}} \mathcal{P}_{\mathbf{p}}(\boldsymbol{\theta}). \quad (4.6)$$

Since we assume that the θ_k are uniformly distributed, the polynomials $P_{p_k}(\theta_k)$ are the corresponding *Legendre polynomial* of degree p_k , according to the Askey scheme (see [52]). The accuracy of the expansion depends on the choice of \mathcal{M} that dictates which polynomials to include in the expansion and on the computation of the coefficients. In [56] an overview on different options is provided.

In this work we use *The Sparse Grids Matlab kit* [56, 57], a Matlab package that, among others, provides an implementation of the gPCE based on sparse grids collocation. Roughly speaking, the package provides first an approximation of y in terms of a linear combination of Lagrange interpolants based at sparse grids [58]. Subsequently, a change of basis is performed to convert this polynomial approximation to a linear combination of suitable ρ -orthogonal polynomials, see [56] for the details of the procedure.

The Sobol indices can then be computed directly from the expansion coefficients as briefly recalled in the following (see [39] for the details). First, let $|\mathcal{M}|$ be the cardinality of \mathcal{M} and assume a well-defined ordering on \mathcal{M} such that \mathbf{p}^i refers to the i -th multi-index; assume for the purposes of notation that this ordering is initialized at 0. Recalling (4.5) one may promptly verify the following expression for the expected value and variance of \tilde{y} :

$$\mathbb{E}[\tilde{y}(\boldsymbol{\theta})] = d_{\mathbf{p}^0}, \quad \text{Var}[\tilde{y}(\boldsymbol{\theta})] = \mathbb{E}[\tilde{y}(\boldsymbol{\theta})^2] - \mathbb{E}[\tilde{y}(\boldsymbol{\theta})]^2 = \sum_{i=1}^{|\mathcal{M}|-1} d_{\mathbf{p}^i}^2.$$

Then, let $\mathcal{M}_k = \{\mathbf{p} \in \mathcal{M} \mid p_k \neq 0\}$, that is, the subset of multi-indices such that the degree of the approximating polynomial corresponding to the variable θ_k is nonzero. The k -th Total Sobol Index S_k^T quantifies the contribution of the k -th parameter combined with the others to the total variance of \tilde{y} and is given by:

$$S_k^T = \frac{\sum_{\mathbf{p} \in \mathcal{M}_k} d_{\mathbf{p}}^2}{\sum_{i=1}^{|\mathcal{M}|-1} d_{\mathbf{p}^i}^2}. \quad (4.7)$$

Similarly, let $\overline{\mathcal{M}}_k = \{\mathbf{p} \in \mathcal{M} \mid p_j = 0 \ \forall j \neq k\}$. The k -th *first-order Sobol index* S_k can be expressed as:

$$S_k = \frac{\sum_{\mathbf{p} \in \mathcal{M}_k \cap \overline{\mathcal{M}}_k} d_{\mathbf{p}}^2}{\sum_{i=1}^{|\mathcal{M}|-1} d_{\mathbf{p}^i}^2}. \quad (4.8)$$

It accounts for the contribution of the k -th parameter alone to the variance of the output.

Remark 4.1. We remark once more that the Sobol indices are defined independently of the gPCE [50]. The decision to introduce them here directly through the gPCE was a practical one, motivated by the fact that the software package *The Sparse Grids Matlab* kit that we employ in this work implements the formulas reported above. However, it is worth remarking that this method to compute Sobol indices is generally very efficient in comparison to sampling techniques based on Monte Carlo algorithms (see [54]). The computational cost is indeed dictated by the number of model simulations required for the computation of the gPCE, which can be contained when using the sparse grids approach, see [56] and references therein. The required algebraic manipulations impact with negligible computational cost. Instead, Monte Carlo based techniques typically require an extensive sampling of the parameter space and thus a large number of model simulations.

Remark 4.2. The numerical simulation of the HOPE model requires suitable schemes that have been optimized and are available as black-box solvers [38, 37]. As hinted above, a local sensitivity analysis that requires manipulating the system equations would not be possible here, as it would also require having access and modifying the code. Hence, performing a Sobol sensitivity analysis allows to call the numerical solver black-box for different values of the input parameters. Note that *The Sparse Grids Matlab* kit can be very easily interfaced with third-party software [56], making the implementation of the global sensitivity analysis quite straightforward.

4.2 Simulation study: U.S. national-level model

Over the intervention period 2023-2030, the sample spaces for PrEP coverage in each group corresponds to the following numbers of persons PrEP in each group:

$$\begin{aligned}\Gamma_{msm} &= [385,000, 775,000], & \Gamma_{hetf} &= [31,600, 465,000], \\ \Gamma_{hetm} &= [29,800, 435,000], & \Gamma_{pwid} &= [10,400, 140,000],\end{aligned}$$

with these numbers based on PrEP eligibility guidelines [11]. We note that, while HOPE model inputs are provided in terms of percent-coverage in each group, we elect to report overall numbers here to avoid ambiguities arising from the definition of PrEP-eligibility, which has been subject to revision in recent years [19, 17].

For each sampled PrEP uptake level, $\theta^{(i)} \in \Gamma$, we run the HOPE model, generating four corresponding model outputs $y_j^{(i)}$ giving the annual HIV incidence (4.4) in each transmission group, i.e. $y_j^{(i)} = I_j^{\text{year}}(\theta^{(i)})$. We stress that we *only* vary PrEP-related parameters; all other parameters in HOPE are kept fixed. Thus, variation in the output ensemble is entirely attributable to differences in levels of PrEP across the ensemble members, and the Sobol indices allow us to quantify the direct and spillover effects of PrEP when given to different transmission groups. We note that, as a variance-based measure, quantifying spillover with Sobol indices no longer provides the direct in terms of NNT offered by the methods used for models (2.1), (3.1).

For each intervention year, we computed the Sobol indices for incidence. The results are plotted in Fig. 4.1. By definition, the indices are normalized. At each time point, the indices give the percentage of the variance in simulated incidence explained by the PrEP uptake in each respective group.

We observe similar dynamics as in the other models. In particular, there does not appear to be any spillover effect for MSM, and 100% of the variance in MSM is explained solely by PrEP uptake among MSM, over the entire time period. For HETF, initially direct PrEP uptake among HETF has the most influence on HETF incidence, however, this changes over time. By the end of the time period, PrEP uptake among MSM is responsible for over 80% of the variance in HETF incidence. For HETM, we also observe significant spillover effects from MSM, however, over a much longer time scale. For the majority of the time period, the direct effect of PrEP uptake among HETM is the most important factor in HETM incidence, however, by the end of the time period, PrEP uptake among MSM becomes more important. While PWID were not considered in the previous models, we note that this group showed similar dynamics to MSM, in that no direct spillover effects were observed.

The results suggest that, despite their simplicity, (2.1) and (3.1) accurately capture the relevant dynamics for studying the effects of PrEP uptake on incidence generally, including the effects of spillover. Nonetheless, we remark that the HOPE spillover results cannot be compared directly to those derived in Sections 2.3 and 3.3. As noted previously, the quantities obtained by solving the spillover systems have physical units and a clear physical meaning: in particular, they give the infections prevented per person on PrEP. Furthermore, their reciprocal corresponds to the number needed to treat, or the number of persons on PrEP necessary to prevent one infection. However, as the equation (4.7) suggests, the Sobol indices are unitless. Therefore, while they have a physical meaning in terms of percentage of the variance explained by each parameter, this is independent of the actual size of variation. Therefore, directly relating Sobol indices to physical quantities, such as number of infections prevented, is not straightforward; the parameter space reduction / aggregation techniques proposed in [22] may provide a possible strategy.

Furthermore, the quantities derived in Sections 2.2 and 3.2 describe the *local* dependence of HIV incidence on PrEP uptake. In fact, for differing levels of baseline PrEP use, we would expect the calculated spillover and NNT to be different in general. In contrast, the Sobol indices describe the *global* dependence of HIV incidence on PrEP uptake; they are constructed by considering variance in HIV incidence over the entire range of PrEP uptake levels. Therefore, these will not change when baseline PrEP uptake levels are varied. For this reason, the Sobol indices are often used in applications to identify the most influential parameters in a parameterized system, see e.g. [40].

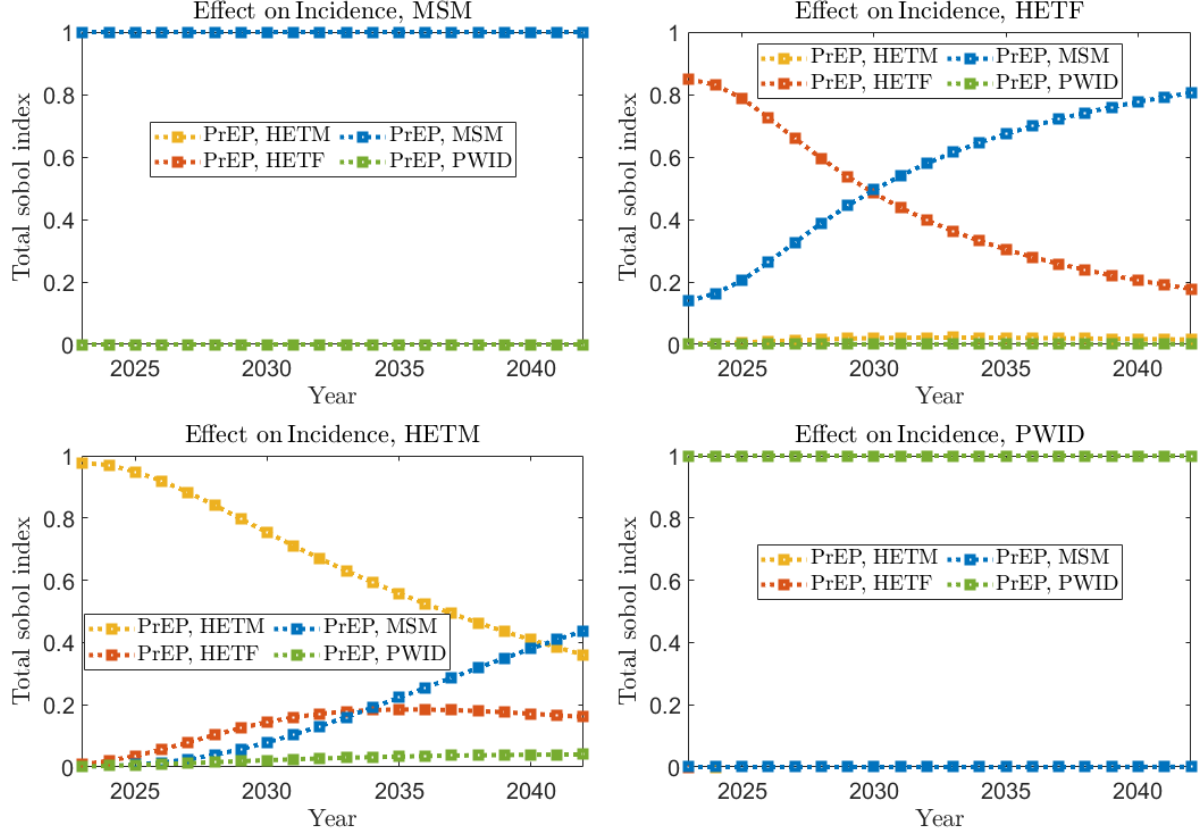


Figure 4.1: HOPE model, Georgia simulation study: Total Sobol indices.

5 Conclusion

In this work, we explored the effects of PrEP on HIV incidence among distinct HIV transmission groups. In particular, we observed how giving PrEP to a particular transmission group affects HIV incidence not only in that group, but in other transmission groups as well, the so-called “spillover effect”. We introduced and analyzed two simplified models of sexual HIV transmission: a three-population version (i.e., the basic model), considering MSM, HETF, and HETM, and a four-population version (i.e., the risk-structured model), which further stratifies the HETF population into high- and low-risk categories. Both models were rigorously analyzed to gain insight into their qualitative features. The analyses revealed that the disease-free equilibria of the models are locally asymptotically stable whenever the associated control reproduction number is less than one. Furthermore, for the special cases of both models (i.e., with no disease-induced mortality), the disease-free equilibrium is shown to be globally asymptotically stable when the control reproduction number is less than one. We demonstrated that, from these simple models, it is possible to derive additional systems which can be used to quantify the spillover effect and NNT directly. A series of numerical simulations on both models showed that the effectiveness of PrEP in preventing new HIV infections varies widely across transmission groups. Furthermore, simulation of the derived spillover models showed that spillovers effects may be significant and show non-trivial temporal dynamics.

The results from the three-population model suggested, for example, that delivering PrEP to MSM was a more effective way to reduce incidence among HETF than delivering PrEP to HETF directly. The results of the risk-structured

model, however, demonstrated that interventions aimed at targeting specific, high-risk populations may change these conclusions somewhat. When PrEP is delivered to high-risk HETF populations, the effect on reducing HETF incidence is larger than the spillover effect from MSM. Furthermore, the spillover effect on HETM incidence from PrEP delivery to high-risk HETF was larger than the direct effect PrEP uptake among HETM. Finally, both models show significant spillover from MSM on all other groups, but no spillover effects among MSM were observed resulting from PrEP delivery in other transmission groups.

We then showed that, while the analytic approaches used on the two simplified models are likely untenable for large-scale, realistic models of HIV transmission, one can still analyze spillover effects on such models through numerical approaches. We considered the HOPE model and performed a variance-based Sobol sensitivity analysis to assess the influence of PrEP delivery across transmission groups on annual HIV incidence in each respective group. The results of this analysis are consistent with the findings obtained with the simplified models, establishing the validity of the simplified model in studying the effects of PrEP delivery to transmission groups.

The current work has several limitations. Notably, all the considered models stratify the populations by transmission group. However, there are other important population stratifications, including age, race/ethnicity, and geographic region, among others. Including these factors may be important for programmatic applications, as spillover effects likely also exist across other population groupings. Additionally, the current models, for simplicity, considered PrEP as completely effective, and perfect adherence among individuals on PrEP. In practice, this may not be the case, and a more complex treatment of PrEP, including further compartmentalization, may further improve the usefulness of the model. Additionally, applying parameter reduction techniques, such as those shown in [22], may help in concretely connecting the spillover dynamics observed in system outputs to model inputs, to aid in planning targeted interventions. Finally, extending the scope of the study to include more populations and regions, such as the EHE jurisdictions, may be valuable for future intervention planning.

Our analysis shows that spillover effects are significant in PrEP delivery interventions. In several instances, we found that spillover provided the most efficient way of reducing HIV incidence within a group. Our study suggests that interventions based on PrEP must take spillover effects into account. Furthermore, calculations based directly on HIV incidence and PrEP data among groups that do not account for spillover effects may provide misleading conclusions. These results suggest that there is significant potential in leveraging spillover effects, and that doing so may provide larger reductions in HIV incidence at reduced cost.

Acknowledgments

The authors would like to thank John Brooks, Nidhi Khurana, Paul Farnham, and Zhao Kun for their constructive input. ABG acknowledges the support, in part, of the National Science Foundation (Grant Number: DMS-2052363; transferred to DMS-2330801). Chiara Piazzola acknowledges the support of the Alexander von Humboldt foundation. Chiara Piazzola is a member of the Gruppo Nazionale Calcolo Scientifico-Istituto Nazionale di Alta Matematica (GNCS-INdAM).

A Mathematical analysis of the three-group model

Before proving Theorem 2.3, it is necessary to establish the following intermediate result.

Theorem A.1. *Consider the basic model (2.1) with $\delta_{msm} = \delta_{hetf} = \delta_{hetm} = 0$ and non-negative initial conditions. The region Ω^* given in (2.7) is positively-invariant and attracts all solutions of the model.*

Proof. Since $N(t) \leq \Pi/\mu$ for all t in Ω^* , it follows from the first equation of the basic model (2.1) that:

$$\frac{dS_{msm}}{dt} \leq \Pi_{msm} - \mu S_{msm} \leq \mu \left(\frac{\Pi_{msm}}{\mu} - S_{msm} \right) \leq \mu(S_{msm}^* - S_{msm}).$$

Hence, if $S_{msm}(t) > S_{msm}^*$, then $\frac{dS_{msm}}{dt} < 0$.

Using similar approach for the third and fifth equations of the model (2.1) we get the following bounds:

$$\frac{dS_{hetf}}{dt} \leq \mu(S_{hetf}^* - S_{hetf}), \quad \frac{dS_{hetm}}{dt} \leq \mu(S_{hetm}^* - S_{hetm}),$$

respectively. Similarly, we have $S_{hetf}(t) \leq S_{hetf}^*$ for all t , provided that $S_{hetf}(0) \leq S_{hetf}^*$, and $S_{hetm}(t) \leq S_{hetm}^*$ for all t , provided that $S_{hetm}(0) \leq S_{hetm}^*$. We can thus conclude that the region Ω^* is positively-invariant. Additionally,

note that: (2.1):

$$\Omega^* = \{ (S_{msm}, I_{msm}, S_{hetf}, I_{hetf}, S_{hetm}, I_{hetm}) \in \Omega : S_{msm} \leq S_{msm}^*, S_{hetf} \leq S_{hetf}^*, S_{hetm} \leq S_{hetm}^* \},$$

which, when combined with positive invariance, establishes attractivity. \square

Then, the proof of Theorem 2.3 follows.

Proof of Theorem 2.3. Consider the basic model (2.1) with $\delta_{msm} = \delta_{hetf} = \delta_{hetm} = 0$. We also assume that $\widehat{\mathbb{R}}_c < 1$. The proof is also based on using a comparison theorem [41, 59, 60, 61]. The equations for the infected compartments of the special case of the model (2.1) can be re-written as:

$$\frac{d}{dt} \begin{bmatrix} I_{msm}(t) \\ I_{hetf}(t) \\ I_{hetm}(t) \end{bmatrix} = (F - \hat{V}) \begin{bmatrix} I_{msm}(t) \\ I_{hetf}(t) \\ I_{hetm}(t) \end{bmatrix} - M \begin{bmatrix} I_{msm}(t) \\ I_{hetf}(t) \\ I_{hetm}(t) \end{bmatrix}, \quad (\text{A.1})$$

where the next generation matrix F is defined in Section 2.1.1 and \hat{V} has the following form:

$$\hat{V} = \begin{bmatrix} \mu & 0 & 0 \\ 0 & \mu & 0 \\ 0 & 0 & \mu \end{bmatrix}.$$

The matrix M is defined as:

$$M = \begin{bmatrix} m_{11} & m_{12} & 0 \\ m_{21} & 0 & m_{23} \\ 0 & m_{32} & 0 \end{bmatrix},$$

with,

$$\begin{aligned} m_{11} &= (S_{msm}^* - S_{msm})a_{msm}(1 - \varepsilon_{msm})\eta_{msm}\beta_M^M, & m_{12} &= (S_{msm}^* - S_{msm})a_{msm}(1 - \varepsilon_{msm})(1 - \eta_{msm})\beta_F^M, \\ m_{21} &= (S_{hetf}^* - S_{hetf})a_{hetf}(1 - \varepsilon_{hetf})\beta_M^F\alpha_{hetf}, & m_{23} &= (S_{hetf}^* - S_{hetf})a_{hetf}(1 - \varepsilon_{hetf})(1 - \alpha_{hetf}), \\ m_{32} &= (S_{hetm}^* - S_{hetm})a_{hetm}(1 - \varepsilon_{hetm})\beta_F^M. \end{aligned}$$

Since $S_{msm} \leq S_{msm}^*, S_{hetf} \leq S_{hetf}^*, S_{hetm} \leq S_{hetm}^*$ for all $t > 0$ in Ω^* (as shown above) and thus (A.1) can be re-written in terms of the following inequality:

$$\frac{d}{dt} \begin{bmatrix} I_{msm}(t) \\ I_{hetf}(t) \\ I_{hetm}(t) \end{bmatrix} \leq (F - \hat{V}) \begin{bmatrix} I_{msm}(t) \\ I_{hetf}(t) \\ I_{hetm}(t) \end{bmatrix}. \quad (\text{A.2})$$

It should be recalled from the local asymptotic stable result for the disease-free equilibrium of the basic model (2.1) (given in Theorem 2.2) that all eigenvalues of the associated next-generation matrix FV^{-1} are negative if $\mathbb{R}_c < 1$ (i.e., $F - V$ is a stable matrix). It follows that the eigenvalues of the next-generation matrix $F\hat{V}^{-1}$, associated with this special case of the basic model (2.1), are also negative if $\widehat{\mathbb{R}}_c < 1$ (i.e., $F - \hat{V}$ is also a stable matrix). Thus, the linearized differential inequality system (A.2) is stable whenever $\rho(F\hat{V}^{-1}) < 1$. Consequently [62, 61, 60, 59, 63].

$$(I_{msm}(t), I_{hetf}(t), I_{hetm}(t)) \rightarrow (0, 0, 0), \text{ as } t \rightarrow \infty.$$

Substituting $I_{msm}(t) = I_{hetf}(t) = I_{hetm}(t) = 0$ into the differential equations for the rate of change of the $S_{msm}(t), S_{hetf}(t)$ and $S_{hetm}(t)$ compartments of the basic model (2.1) shows that:

$$S_{msm}(t) \rightarrow S_{msm}^*, S_{hetf}(t) \rightarrow S_{hetf}^* \text{ and } S_{hetm}(t) \rightarrow S_{hetm}^* \text{ as } t \rightarrow \infty.$$

Thus, the disease-free equilibrium \mathcal{E}_0 of the special case of the basic model (2.1), with $\delta_{msm} = \delta_{hetf} = \delta_{hetm} = 0$ is globally-asymptotically stable in Ω^* whenever $\widehat{\mathbb{R}}_c < 1$. \square

B Relaxing the assumption on disease-induced mortality

As mentioned in Section 2.2.1, we assumed that $\delta_j = 0$ in order to simplify the derivation of the spillover equations. In practice, the general case $\delta_j \neq 0$ can be considered.

Note that, if the $\delta_j \neq 0$, then the Λ_j are affected due to the presence of the N_j terms (2.20) due to differences in the perturbed total populations \hat{N}_j and non-perturbed populations N_j . When mortality rates are equal in the S and I compartments, the overall number of persons does not depend on the allocation of the population within each compartment; however, if the mortality rates differ (for instance, when $\delta_j \neq 0$), this is no longer the case. To see this, adding a generic S_j and I_j compartment, one obtains the following differential equation for N_j :

$$\frac{dN_j}{dt} = \Pi_j - \mu S_j - (\mu + \delta_j) I_j = \Pi_j - \mu N_j - \delta_j I_j.$$

Consequently, (2.28) now reads:

$$\begin{aligned} -\left(\hat{\Lambda}_j^T \hat{\mathbf{X}}\right) \hat{S}_j + \left(\Lambda_j^T \mathbf{X}\right) S_j &= -\left(\hat{\Lambda}_j^T \left(\hat{\mathbf{X}} - \mathbf{X} + \mathbf{X}\right)\right) \left(\hat{S}_j - S_j + S_j\right) + \left(\Lambda_j^T \mathbf{X}\right) S_j \\ &= -\left(\hat{\Lambda}_j^T \left(\hat{\mathbf{X}} - \mathbf{X}\right)\right) \left(\hat{S}_j - S_j\right) - \left(\hat{\Lambda}_j^T \hat{\mathbf{X}}\right) \left(\hat{S}_j - S_j\right) \\ &\quad - \left(\hat{\Lambda}_j^T \left(\hat{\mathbf{X}} - \mathbf{X}\right)\right) \hat{S}_j - \left(\left(\hat{\Lambda}_j - \Lambda_j\right)^T \mathbf{X}\right) S_j. \end{aligned}$$

As $\hat{\Lambda}_j \rightarrow \Lambda_j$ as $\tilde{\varepsilon} \rightarrow 0$ (we use the symbol $\tilde{\varepsilon}$ to denote the perturbation to the PrEP fraction among the population group k), dividing by $\tilde{\varepsilon}$ and taking the limit as $\tilde{\varepsilon} \rightarrow 0$ gives:

$$\lim_{\tilde{\varepsilon} \rightarrow 0} \frac{-\left(\hat{\Lambda}_j^T \hat{\mathbf{X}}\right) \hat{S}_j + \left(\Lambda_j^T \mathbf{X}\right) S_j}{\tilde{\varepsilon}} = -\left(\Lambda_j^T \mathbf{X}\right) \sigma_j - \left(\Lambda_j^T \boldsymbol{\vartheta}\right) \hat{S}_j - \left(\lim_{\tilde{\varepsilon} \rightarrow 0} \frac{\left(\hat{\Lambda}_j - \Lambda_j\right)^T \mathbf{X}}{\tilde{\varepsilon}}\right) S_j.$$

We now examine the expression in the limit on the right-hand side above, for $j = msm$. Recalling the symbol definition in (2.20) we can write:

$$\lim_{\tilde{\varepsilon} \rightarrow 0} \frac{\hat{\Lambda}_{msm} - \Lambda_{msm}}{\tilde{\varepsilon}} = \begin{pmatrix} 0 \\ a_{msm} \eta_{msm} \beta_M^M \lim_{\tilde{\varepsilon} \rightarrow 0} \frac{1}{\tilde{\varepsilon}} \left(\frac{1}{\hat{N}_{msm}} - \frac{1}{N_{msm}} \right) \\ 0 \\ a_{msm} (1 - \eta_{msm}) \beta_F^M \lim_{\tilde{\varepsilon} \rightarrow 0} \frac{1}{\tilde{\varepsilon}} \left(\frac{1}{\hat{N}_{hetf}} - \frac{1}{N_{hetf}} \right) \\ 0 \\ 0 \end{pmatrix} \quad (\text{B.1})$$

The (2, 1) entry on the right-hand side of the spillover system involves the derivative of the inverse population size $1/N_{msm}$ with respect to the perturbation $\tilde{\varepsilon}$. To compute this, we observe that

$$\begin{aligned} \lim_{\tilde{\varepsilon} \rightarrow 0} \frac{1}{\tilde{\varepsilon}} \left(\frac{1}{\hat{N}_{msm}} - \frac{1}{N_{msm}} \right) &= -\lim_{\tilde{\varepsilon} \rightarrow 0} \frac{\hat{N}_{msm} - N_{msm}}{\tilde{\varepsilon}} \cdot \lim_{\tilde{\varepsilon} \rightarrow 0} \frac{1}{N_{msm} \hat{N}_{msm}} \\ &= -\frac{1}{N_{msm}^2} \cdot \lim_{\tilde{\varepsilon} \rightarrow 0} \frac{\hat{N}_{msm} - N_{msm}}{\tilde{\varepsilon}}. \end{aligned} \quad (\text{B.2})$$

Since $\hat{N}_{msm} = \hat{S}_{msm} + \hat{I}_{msm}$ and similarly for N_{msm} , we can write:

$$\hat{N}_{msm} - N_{msm} = (\hat{S}_{msm} - S_{msm}) + (\hat{I}_{msm} - I_{msm}),$$

and by definition of the perturbation derivatives (see (2.9)):

$$\lim_{\tilde{\varepsilon} \rightarrow 0} \frac{\hat{N}_{msm} - N_{msm}}{\tilde{\varepsilon}} = \sigma_{msm}^k + \gamma_{msm}^k.$$

Substituting back into equation (B.2), we find:

$$\lim_{\tilde{\varepsilon} \rightarrow 0} \frac{1}{\tilde{\varepsilon}} \left(\frac{1}{\hat{N}_{msm}} - \frac{1}{N_{msm}} \right) = -\frac{\sigma_{msm}^k + \gamma_{msm}^k}{N_{msm}^2}.$$

The (4, 1) term in (B.1) can be rewritten in a similar way. It thus follows:

$$\lim_{\tilde{\varepsilon} \rightarrow 0} \frac{\hat{\Lambda}_{msm} - \Lambda_{msm}}{\tilde{\varepsilon}} = \begin{pmatrix} 0 \\ a_{msm}\eta_{msm}\beta_M^M \cdot \frac{\sigma_{msm}^k + \gamma_{msm}^k}{N_{msm}^2} \\ 0 \\ a_{msm}(1 - \eta_{msm})\beta_F^M \cdot \frac{\sigma_{hetf}^k + \gamma_{hetf}^K}{N_{hetf}^2} \\ 0 \\ 0 \end{pmatrix} =: \Xi_{msm}^k.$$

Similarly, we define:

$$\Xi_{hetf}^k := \begin{pmatrix} 0 \\ a_{hetf}\alpha_{hetf}\beta_M^F \cdot \frac{\sigma_{msm}^k + \gamma_{msm}^k}{N_{msm}^2} \\ 0 \\ 0 \\ 0 \\ a_{hetf}(1 - \alpha_{hetf})\beta_M^F \cdot \frac{\sigma_{hetm}^k + \gamma_{hetm}^k}{N_{hetm}^2} \end{pmatrix}, \quad \Xi_{hetm}^k := \begin{pmatrix} 0 \\ 0 \\ 0 \\ a_{hetm}\beta_F^M \cdot \frac{\sigma_{hetf}^k + \gamma_{hetf}^k}{N_{hetf}^2} \\ 0 \\ 0 \end{pmatrix}. \quad (\text{B.3})$$

The above computations show that, by adding appropriately signed terms of the form,

$$\left(\Xi_j^{kT} \mathbf{X} \right) S_j \quad (\text{B.4})$$

to the right-hand sides of the systems (2.30), (2.31), and (2.32), we can formally account for the case $\delta_j \neq 0$ while preserving the original system structure; note that, other than the terms (B.4), the remainder of the system is identical to the $\delta_j = 0$ case.

As seen in (B.4), these terms are scaled by inverse squared population sizes, i.e., $1/N_j^2 \ll 1$. As such, the contributions of the terms in (B.4) are substantially smaller than those appearing in (2.30)–(2.32), and their influence on the system dynamics is negligible. Consequently, we adopt the simplified spillover system (2.30)–(2.32) as our working model, with the understanding that it qualitatively approximates the case $\delta_j \neq 0$.

C Mathematical analysis of the risk-structured model

For the risk-structured model (3.1) to be biologically and epidemiologically meaningful, it is instructive to explore its basic qualitative features with respect to its well-posedness (as discussed in Section 2.1). We claim the following result:

Theorem C.1. *Consider the risk-structured model (3.1) with non-negative initial conditions. The region*

$$\Omega_r = \left\{ (S_{msm}, I_{msm}, S_{hetf_h}, I_{hetf_h}, S_{hetf_l}, I_{hetf_l}, S_{hetm}, I_{hetm}) \in \mathbb{R}_+^8 : 0 \leq N \leq \frac{\Pi_r}{\mu} \right\},$$

with $\Pi_r = \Pi_{msm} + \Pi_{hetf_h} + \Pi_{hetf_l} + \Pi_{hetm}$ is positively-invariant and attracts all solutions of the model (3.1).

Proof. Adding all the equations of the risk-structured model (3.1) gives:

$$\frac{dN}{dt} = \Pi_r - \mu N - \delta_{msm} I_{msm} - \delta_{hetf_h} I_{hetf_h} - \delta_{hetf_l} I_{hetf_l} - \delta_{hetm} S_{hetm}.$$

By the non-negativity of parameters for model (3.1), it follows that

$$\frac{dN}{dt} \leq \Pi_r - \mu N.$$

Hence if $N \leq \frac{\Pi_r}{\mu}$, then $\frac{dN}{dt} \leq 0$. Thus, it follows, by applying a standard comparison theorem [41], that:

$$N(t) \leq \frac{\Pi_r}{\mu} + \left[N(0) - \frac{\Pi_r}{\mu} \right] e^{-\mu t}.$$

In particular, $N(t) \leq \frac{\Pi_r}{\mu}$ if $N(0) \leq \frac{\Pi_r}{\mu}$. Further, if $N(t) > \frac{\Pi_r}{\mu}$, then $\frac{dN(t)}{dt} < 0$. Thus, every solution of the risk-structured model (3.1) with initial conditions in Ω_r remains in Ω_r for all time $t > 0$, and those outside Ω_r are eventually attracted into Ω_r . In other words, the region Ω_r is positively-invariant and attracts all initial solutions of the model (3.1). \square

The consequence of Theorem C.1 is that it is sufficient to consider the dynamics of the flow generated by the model (3.1) in Ω_r , where the model is well-posed mathematically and epidemiologically [42].

C.1 Reproduction analysis of the risk-structured model (3.1)

In the following we list the expressions for the quantities H_1, H_2, H_3 , and H_4 that enter in the formula for the control reproduction number in Section 3.1.1:

$$\begin{aligned}
H_1 &= \frac{\sqrt{12 H_5^{1/2} H_8 + 12 H_5^{1/2} H_6^{1/3} H_9 - H_5^{1/2} H_9^2 - 9 H_5^{1/2} H_6^{2/3} - H_4}}{6 H_5^{1/4} H_6^{1/6}}, \\
H_2 &= \frac{\sqrt{12 H_5^{1/2} H_8 + 12 H_5^{1/2} H_6^{1/3} H_9 + H_4 - H_5^{1/2} H_9^2 - 9 H_5^{1/2} H_6^{2/3}}}{6 H_5^{1/4} H_6^{1/6}}, \\
H_3 &= \frac{H_5^{1/2}}{6 H_6^{1/6}}, \quad H_4 = 3\sqrt{6} H_{10} \sqrt{3^{3/2} H_7 + 27 H_{10}^2 - 2 H_9^3 - 72 H_8 H_9}, \\
H_5 &= H_9^2 + 9 H_6^{2/3} + 6 H_9 H_6^{1/3} + \frac{3 f_{11} H_{13}}{K_1^2 K_2 K_3 K_4} + \frac{12 H_{11}}{K_1 K_2 K_3 K_4} - \frac{9 f_{11}^4}{64 K_1^4} - \frac{3 f_{11}^2 H_{12}}{4 K_1^3 K_2 K_3 K_4}, \\
H_6 &= \frac{\sqrt{3} H_7}{18} + \frac{H_{10}^2}{2} - \frac{4 H_8 H_9}{3} - \frac{H_9^3}{27}, \\
H_7 &= \sqrt{256 H_8^3 + 128 H_8^2 H_9^2 + 27 H_{10}^4 + 16 H_8 H_9^4 - 144 H_8 H_9 H_{10}^2 - 4 H_9^3 H_{10}^2}, \\
H_8 &= \frac{3 f_{11}^4}{256 K_1^4} + \frac{f_{11}^2 H_{12}}{16 K_1^3 K_2 K_3 K_4} - \frac{f_{11} H_{13}}{4 K_1^2 K_2 K_3 K_4} - \frac{H_{11}}{K_1 K_2 K_3 K_4}, \\
H_9 &= \frac{3 f_{11}^2}{8 K_1^2} + \frac{H_{12}}{K_1 K_2 K_3 K_4}, \quad H_{10} = \frac{f_{11}^3}{8 K_1^3} + \frac{f_{11} H_{12}}{2 K_1^2 K_2 K_3 K_4} - \frac{H_{13}}{K_1 K_2 K_3 K_4}, \\
H_{11} &= f_{12} f_{21} f_{34} f_{43} + f_{13} f_{24} f_{31} f_{42} - f_{12} f_{24} f_{31} f_{43} - f_{13} f_{21} f_{34} f_{42}, \\
H_{12} &= K_3 K_4 f_{12} f_{21} + K_2 K_4 f_{13} f_{31} + K_1 K_3 f_{24} f_{42} + K_1 K_2 f_{34} f_{43}, \\
H_{13} &= K_3 f_{11} f_{24} f_{42} + K_2 f_{11} f_{34} f_{43}.
\end{aligned}$$

Theorem C.2. *The disease-free equilibrium \mathcal{E}_r of the risk-structured model (3.1) is locally-asymptotically stable if $\mathbb{R}_{cr} < 1$, and unstable if $\mathbb{R}_{cr} > 1$.*

The epidemiological implication of Theorem C.2 is that a small influx of HIV-infected individuals will not generate a large outbreak in the community if the associated control reproduction number ($\mathbb{R}_{cr} < 1$) is brought to, and maintained at a, value less than unity.

C.2 Global asymptotic stability of the disease-free equilibrium: special case

Using the similar approach as used in Section 2.3, we explore extending the result in Theorem C.2 to prove the global asymptotic stability of the disease-free equilibrium for the special case of the risk-structured model (3.1). Consider the model (3.1) with $\delta_{msm} = \delta_{hetf_h} = \delta_{hetf_l} = \delta_{hetm} = 0$ and add the equations for the respective rate of change of populations in the susceptible and infected compartments (i.e., $S_j(t)$ and $I_j(t)$). This shows that $\frac{dN_j(t)}{dt} = \Pi_j - \mu N$, with $j \in \{msm, hetf_h, hetf_l, hetm\}$, from which it follows that $N_j(t) \rightarrow \frac{\Pi_j}{\mu}$ as $t \rightarrow \infty$. From now on, the total sexually active population in group j at time t , denoted by $N_j(t)$, will be replaced by its limiting value, $N_j^{**} = \frac{\Pi_j}{\mu}$ (i.e., here too, the standard incidence formulation is now replaced by a mass action incidence). Consider the following

biologically-feasible region for the special case of the risk-structured model (3.1):

$$\begin{aligned}\Omega_r^{**} &= \{(S_{msm}, I_{msm}, S_{hetfh}, I_{hetfh}, S_{hetfi}, I_{hetfi}, S_{hetm}, I_{hetm}) \in \Omega_r : \\ &S_{msm} \leq S_{msm}^{**}, S_{hetfh} \leq S_{hetfh}^{**}, S_{hetfi} \leq S_{hetfi}^{**}, S_{hetm} \leq S_{hetm}^{**}\}.\end{aligned}$$

It can also be shown that the region Ω_r^* is also positively-invariant and attracting with respect to this special case of the model (as shown in Appendix A). The associated control reproduction number of this special case of the risk-structured model, denoted by $\widehat{\mathbb{R}}_{cr}$, is given by:

$$\widehat{\mathbb{R}}_{cr} = \mathbb{R}_{cr}|_{\delta_{msm}=\delta_{hetfh}=\delta_{hetfi}=\delta_{hetm}=0}.$$

We claim the following result:

Theorem C.3. *Consider the special case of the risk-structured model (3.1) with $\delta_{msm} = \delta_{hetfh} = \delta_{hetfi} = \delta_{hetm} = 0$. The disease-free equilibrium \mathcal{E}_r is globally-asymptotically stable in Ω_r^{**} whenever $\widehat{\mathbb{R}}_{cr} < 1$.*

Proof. We assume that $\widehat{\mathbb{R}}_{cr} < 1$, for the special case of the risk-structured model (3.1), with $\delta_{msm} = \delta_{hetfh} = \delta_{hetfi} = \delta_{hetm} = 0$. It can be shown, that the region Ω_r^{**} is positively-invariant and attracts all solutions of the aforementioned special case of the model (3.1) (similarly to what done in Appendix A for the basic model). Then, the equations for the infected compartments can be re-written in terms of the next generation matrices F_r and \widehat{V}_r (where F_r is as defined in Section C.1 and $\widehat{V}_r|_{V_r=\delta_{msm}=\delta_{hetfh}=\delta_{hetfi}=\delta_{hetm}=0}$) as below:

$$\frac{d}{dt} \begin{bmatrix} I_{msm}(t) \\ I_{hetfh}(t) \\ I_{hetfi}(t) \\ I_{hetm}(t) \end{bmatrix} = (F_r - \widehat{V}_r) \begin{bmatrix} I_{msm}(t) \\ I_{hetfh}(t) \\ I_{hetfi}(t) \\ I_{hetm}(t) \end{bmatrix} - M_r \begin{bmatrix} I_{msm}(t) \\ I_{hetfh}(t) \\ I_{hetfi}(t) \\ I_{hetm}(t) \end{bmatrix}, \quad (\text{C.1})$$

where, the matrix M_r is defined as:

$$M_r = \begin{bmatrix} m_{11_r} & m_{12_r} & m_{13_r} & 0 \\ m_{21_r} & 0 & 0 & m_{24_r} \\ m_{31_r} & 0 & 0 & m_{34_r} \\ 0 & m_{42_r} & m_{43_r} & 0 \end{bmatrix},$$

with,

$$\begin{aligned}m_{11_r} &= (S_{msm}^* - S_{msm})a_{msm}(1 - \varepsilon_{msm})\eta_{msm}\beta_M^M, & m_{12_r} &= (S_{msm}^* - S_{msm})a_{msm}(1 - \varepsilon_{msm})\eta_{hetfh}\beta_F^M, \\ m_{13_r} &= (S_{msm}^* - S_{msm})a_{msm}(1 - \varepsilon_{msm})(1 - \eta_{msm} - \eta_{hetfh})\beta_F^M, \\ m_{21_r} &= (S_{hetfh}^* - S_{hetfh})a_{hetfh}(1 - \varepsilon_{hetfh})\alpha_{hetfh}\beta_M^F, \\ m_{24_r} &= (S_{hetfi}^* - S_{hetfi})a_{hetfh}(1 - \varepsilon_{hetfh})(1 - \alpha_{hetfh})\beta_M^F, \\ m_{31_r} &= (S_{hetfi}^* - S_{hetfi})a_{hetfi}(1 - \varepsilon_{hetfi})\alpha_{hetfi}\beta_M^F, \\ m_{34_r} &= (S_{hetfi}^* - S_{hetfi})a_{hetfi}(1 - \varepsilon_{hetfi})(1 - \alpha_{hetfi})\beta_M^F, & m_{42_r} &= (S_{hetm}^* - S_{hetm})a_{hetm}(1 - \varepsilon_{hetm})\gamma_h\beta_F^M, \\ m_{43_r} &= (S_{hetm}^* - S_{hetm})a_{hetm}(1 - \varepsilon_{hetm})(1 - \gamma_h)\beta_F^M.\end{aligned}$$

Since $S_{msm} \leq S_{msm}^{**}$, $S_{hetfh} \leq S_{hetfh}^{**}$, $S_{hetfi} \leq S_{hetfi}^{**}$ and $S_{hetm} \leq S_{hetm}^{**}$ for all $t > 0$ in Ω_r^{**} . Thus, it follows that the matrix M_r is non-negative. Hence, (C.1) can be re-written in terms of the following inequality:

$$\frac{d}{dt} \begin{bmatrix} I_{msm}(t) \\ I_{hetfh}(t) \\ I_{hetfi}(t) \\ I_{hetm}(t) \end{bmatrix} \leq (F_r - \widehat{V}_r) \begin{bmatrix} I_{msm}(t) \\ I_{hetfh}(t) \\ I_{hetfi}(t) \\ I_{hetm}(t) \end{bmatrix}.$$

The proof is concluded the same way as in the proof of Theorem 2.3. Thus, the disease-free equilibrium \mathcal{E}_r of the special case of the risk-structured model (3.1) with $\delta_{msm} = \delta_{hetfh} = \delta_{hetfi} = \delta_{hetm} = 0$ is globally-asymptotically stable in Ω_r^{**} whenever $\widehat{\mathbb{R}}_{cr} < 1$. \square

D Additional risk-stratified spillover equations

Here the spillover equations for the model (3.1) are provided when giving PrEP to hi-risk HETF, low-risk HETF, and HETM, in the following equations (D.1), (D.2), and (D.3), respectively.

$$\left\{ \begin{array}{l} \frac{d\sigma_{msm}^{hetf_h}}{dt} = -(1 - \varepsilon_{msm}) \left[\left(\Lambda_{msm}^T \vartheta^{hetf_h} \right) S_{msm} \right] + \left(\Lambda_{msm}^T \mathbf{X} \right) \sigma_{msm}^{hetf_h} - \mu \sigma_{msm}^{hetf_h}, \\ \frac{d\gamma_{msm}^{hetf_h}}{dt} = (1 - \varepsilon_{msm}) \left[\left(\Lambda_{msm}^T \vartheta^{hetf_h} \right) S_{msm} + \left(\Lambda_{msm}^T \mathbf{X} \right) \sigma_{msm}^{hetf_h} \right] - \mu \gamma_{msm}^{hetf_h}, \\ \frac{d\sigma_{hetf_h}^{hetf_h}}{dt} = -(1 - \varepsilon_{hetf_h}) \left[\left(\Lambda_{hetf_h}^T \vartheta^{hetf_h} \right) S_{hetf_h} + \left(\Lambda_{hetf_h}^T \mathbf{X} \right) \sigma_{hetf_h}^{hetf_h} \right] + \left(\Lambda_{hetf_h}^T \mathbf{X} \right) S_{hetf_h} - \mu \sigma_{hetf_h}^{hetf_h}, \\ \frac{d\gamma_{hetf_h}^{hetf_h}}{dt} = (1 - \varepsilon_{hetf_h}) \left[\left(\Lambda_{hetf_h}^T \vartheta^{hetf_h} \right) S_{hetf_h} + \left(\Lambda_{hetf_h}^T \mathbf{X} \right) \sigma_{hetf_h}^{hetf_h} \right] - \left(\Lambda_{hetf_h}^T \mathbf{X} \right) S_{hetf_h} - \mu \gamma_{hetf_h}^{hetf_h}, \\ \frac{d\sigma_{hetf_l}^{hetf_h}}{dt} = -(1 - \varepsilon_{hetf_l}) \left[\left(\Lambda_{hetf_l}^T \vartheta^{hetf_h} \right) S_{hetf_l} + \left(\Lambda_{hetf_l}^T \mathbf{X} \right) \sigma_{hetf_l}^{hetf_h} \right] - \mu \sigma_{hetf_l}^{hetf_h}, \\ \frac{d\gamma_{hetf_l}^{hetf_h}}{dt} = (1 - \varepsilon_{hetf_l}) \left[\left(\Lambda_{hetf_l}^T \vartheta^{hetf_h} \right) S_{hetf_l} + \left(\Lambda_{hetf_l}^T \mathbf{X} \right) \sigma_{hetf_l}^{hetf_h} \right] - \mu \gamma_{hetf_l}^{hetf_h}, \\ \frac{d\sigma_{hetm}^{hetf_h}}{dt} = -(1 - \varepsilon_{hetm}) \left[\left(\Lambda_{hetm}^T \vartheta^{hetf_h} \right) S_{hetm} + \left(\Lambda_{hetm}^T \mathbf{X} \right) \sigma_{hetm}^{hetf_h} \right] - \mu \sigma_{hetm}^{hetf_h}, \\ \frac{d\gamma_{hetm}^{hetf_h}}{dt} = (1 - \varepsilon_{hetm}) \left[\left(\Lambda_{hetm}^T \vartheta^{hetf_h} \right) S_{hetm} + \left(\Lambda_{hetm}^T \mathbf{X} \right) \sigma_{hetm}^{hetf_h} \right] - \mu \gamma_{hetm}^{hetf_h}. \end{array} \right. \quad (D.1)$$

$$\left\{ \begin{array}{l} \frac{d\sigma_{msm}^{hetf_l}}{dt} = -(1 - \varepsilon_{msm}) \left[\left(\Lambda_{msm}^T \vartheta^{hetf_l} \right) S_{msm} + \left(\Lambda_{msm}^T \mathbf{X} \right) \sigma_{msm}^{hetf_l} \right] - \mu \sigma_{msm}^{hetf_l}, \\ \frac{d\gamma_{msm}^{hetf_l}}{dt} = (1 - \varepsilon_{msm}) \left[\left(\Lambda_{msm}^T \vartheta^{hetf_l} \right) S_{msm} + \left(\Lambda_{msm}^T \mathbf{X} \right) \sigma_{msm}^{hetf_l} \right] - \mu \gamma_{msm}^{hetf_l}, \\ \frac{d\sigma_{hetf_h}^{hetf_l}}{dt} = -(1 - \varepsilon_{hetf_h}) \left[\left(\Lambda_{hetf_h}^T \vartheta^{hetf_l} \right) S_{hetf_h} + \left(\Lambda_{hetf_h}^T \mathbf{X} \right) \sigma_{hetf_h}^{hetf_l} \right] - \mu \sigma_{hetf_h}^{hetf_l}, \\ \frac{d\gamma_{hetf_h}^{hetf_l}}{dt} = (1 - \varepsilon_{hetf_h}) \left[\left(\Lambda_{hetf_h}^T \vartheta^{hetf_l} \right) S_{hetf_h} + \left(\Lambda_{hetf_h}^T \mathbf{X} \right) \sigma_{hetf_h}^{hetf_l} \right] - \mu \gamma_{hetf_h}^{hetf_l}, \\ \frac{d\sigma_{hetf_l}^{hetf_l}}{dt} = -(1 - \varepsilon_{hetf_l}) \left[\left(\Lambda_{hetf_l}^T \vartheta^{hetf_l} \right) S_{hetf_l} + \left(\Lambda_{hetf_l}^T \mathbf{X} \right) \sigma_{hetf_l}^{hetf_l} \right] + \left(\Lambda_{hetf_l}^T \mathbf{X} \right) S_{hetf_l} - \mu \sigma_{hetf_l}^{hetf_l}, \\ \frac{d\gamma_{hetf_l}^{hetf_l}}{dt} = (1 - \varepsilon_{hetf_l}) \left[\left(\Lambda_{hetf_l}^T \vartheta^{hetf_l} \right) S_{hetf_l} + \left(\Lambda_{hetf_l}^T \mathbf{X} \right) \sigma_{hetf_l}^{hetf_l} \right] - \left(\Lambda_{hetf_l}^T \mathbf{X} \right) S_{hetf_l} - \mu \gamma_{hetf_l}^{hetf_l}, \\ \frac{d\sigma_{hetm}^{hetf_l}}{dt} = -(1 - \varepsilon_{hetm}) \left[\left(\Lambda_{hetm}^T \vartheta^{hetf_l} \right) S_{hetm} + \left(\Lambda_{hetm}^T \mathbf{X} \right) \sigma_{hetm}^{hetf_l} \right] - \mu \sigma_{hetm}^{hetf_l}, \\ \frac{d\gamma_{hetm}^{hetf_l}}{dt} = (1 - \varepsilon_{hetm}) \left[\left(\Lambda_{hetm}^T \vartheta^{hetf_l} \right) S_{hetm} + \left(\Lambda_{hetm}^T \mathbf{X} \right) \sigma_{hetm}^{hetf_l} \right] - \mu \gamma_{hetm}^{hetf_l}. \end{array} \right. \quad (D.2)$$

$$\left\{ \begin{array}{l}
\frac{d\sigma_{msm}^{hetm}}{dt} = -(1 - \varepsilon_{msm}) \left[\left(\Lambda_{msm}^T \vartheta^{hetm} \right) S_{msm} + \left(\Lambda_{msm}^T \mathbf{X} \right) \sigma_{msm}^h \right] - \mu \sigma_{msm}^{hetm}, \\
\frac{d\gamma_{msm}^{hetm}}{dt} = (1 - \varepsilon_{msm}) \left[\left(\Lambda_{msm}^T \vartheta^{hetm} \right) S_{msm} + \left(\Lambda_{msm}^T \mathbf{X} \right) \sigma_{msm}^{hetm} \right] - \mu \gamma_{msm}^{hetm}, \\
\frac{d\sigma_{hetfh}^{hetm}}{dt} = -(1 - \varepsilon_{hetfh}) \left[\left(\Lambda_{hetfh}^T \vartheta^{hetm} \right) S_{hetfh} + \left(\Lambda_{hetfh}^T \mathbf{X} \right) \sigma_{hetfh}^h \right] - \mu \sigma_{hetfh}^{hetm}, \\
\frac{d\gamma_{hetfh}^{hetm}}{dt} = (1 - \varepsilon_{hetfh}) \left[\left(\Lambda_{hetfh}^T \vartheta^{hetm} \right) S_{hetfh} + \left(\Lambda_{hetfh}^T \mathbf{X} \right) \sigma_{hetfh}^{hetm} \right] - \mu \gamma_{hetfh}^{hetm}, \\
\frac{d\sigma_{hetfi}^{hetm}}{dt} = -(1 - \varepsilon_{hetfi}) \left[\left(\Lambda_{hetfi}^T \vartheta^{hetm} \right) S_{hetfi} + \left(\Lambda_{hetfi}^T \mathbf{X} \right) \sigma_{hetfi}^h \right] - \mu \sigma_{hetfi}^{hetm}, \\
\frac{d\gamma_{hetfi}^{hetm}}{dt} = (1 - \varepsilon_{hetfi}) \left[\left(\Lambda_{hetfi}^T \vartheta^{hetm} \right) S_{hetfi} + \left(\Lambda_{hetfi}^T \mathbf{X} \right) \sigma_{hetfi}^{hetm} \right] - \mu \gamma_{hetfi}^{hetm}, \\
\frac{d\sigma_{hetm}^{hetm}}{dt} = -(1 - \varepsilon_{hetm}) \left[\left(\Lambda_{hetm}^T \vartheta^{hetm} \right) S_{hetm} + \left(\Lambda_{hetm}^T \mathbf{X} \right) \sigma_{hetm}^{hetm} \right] + \left(\Lambda_{hetm}^T \mathbf{X} \right) S_{hetm} - \mu \sigma_{hetm}^{hetm}, \\
\frac{d\gamma_{hetm}^{hetm}}{dt} = (1 - \varepsilon_{hetm}) \left[\left(\Lambda_{hetm}^T \vartheta^{hetm} \right) S_{hetm} + \left(\Lambda_{hetm}^T \mathbf{X} \right) \sigma_{hetm}^{hetm} \right] - \left(\Lambda_{hetm}^T \mathbf{X} \right) S_{hetm} - \mu \gamma_{hetm}^{hetm}.
\end{array} \right. \quad (D.3)$$

References

- [1] Centers for Disease Control and Prevention. CDC Statement on FDA Approval of Drug for HIV Prevention, 2012.
- [2] Centers for Disease Control and Prevention. NCHHSTP AtlasPlus , 2023.
- [3] Sheena McCormack, David T Dunn, Monica Desai, David I Dolling, Mitzy Gafos, Richard Gilson, Ann K Sullivan, Amanda Clarke, Iain Reeves, Gabriel Schembri, et al. Pre-exposure prophylaxis to prevent the acquisition of HIV-1 infection (PROUD): effectiveness results from the pilot phase of a pragmatic open-label randomised trial. *The Lancet*, 387(10013):53–60, 2016.
- [4] Robert M Grant, Javier R Lama, Peter L Anderson, Vanessa McMahan, Albert Y Liu, Lorena Vargas, Pedro Goicochea, Martín Casapía, Juan Vicente Guanira-Carranza, Maria E Ramirez-Cardich, et al. Preexposure chemoprophylaxis for HIV prevention in men who have sex with men. *New England Journal of Medicine*, 363(27):2587–2599, 2010.
- [5] Robert M Grant, Peter L Anderson, Vanessa McMahan, Albert Liu, K Rivet Amico, Megha Mehrotra, Sybil Hosek, Carlos Mosquera, Martin Casapia, Orlando Montoya, et al. Uptake of pre-exposure prophylaxis, sexual practices, and HIV incidence in men and transgender women who have sex with men: a cohort study. *The Lancet infectious diseases*, 14(9):820–829, 2014.
- [6] Albert Y Liu, Stephanie E Cohen, Eric Vittinghoff, Peter L Anderson, Susanne Doblecki-Lewis, Oliver Bacon, Wairimu Chege, Brian S Postle, Tim Matheson, K Rivet Amico, et al. Preexposure prophylaxis for HIV infection integrated with municipal-and community-based sexual health services. *JAMA internal medicine*, 176(1):75–84, 2016.
- [7] Julia L Marcus, Leo B Hurley, Dong Phuong Nguyen, Michael J Silverberg, and Jonathan E Volk. Redefining human immunodeficiency virus (HIV) preexposure prophylaxis failures. *Clinical Infectious Diseases*, 65(10):1768–1769, 2017.
- [8] Jonathan E Volk, Julia L Marcus, Tony Phengrasamy, Derek Blechinger, Dong Phuong Nguyen, Stephen Follansbee, and C Bradley Hare. No new HIV infections with increasing use of HIV preexposure prophylaxis in a clinical practice setting. *Clinical infectious diseases*, 61(10):1601–1603, 2015.
- [9] Kachit Choopanya, Michael Martin, Pravan Suntharasamai, Udomsak Sangkum, Philip A Mock, Manoj Leethochawalit, Sithisat Chiamwongpaet, Praphan Kitisin, Pitinan Natrujirote, Somyot Kittimunkong, et al. Antiretroviral prophylaxis for HIV infection in injecting drug users in Bangkok, Thailand (the Bangkok Tenofovir Study): a randomised, double-blind, placebo-controlled phase 3 trial. *The Lancet*, 381(9883):2083–2090, 2013.

- [10] Michael Martin, Suphak Vanichseni, Pravan Suntharasamai, Udomsak Sangkum, Philip A Mock, Manoj Leethochawalit, Sithisat Chiamwongpaet, Marcel E Curlin, Supawadee Na-Pompet, Anchalee Warapron-mongkholkul, et al. The impact of adherence to preexposure prophylaxis on the risk of HIV infection among people who inject drugs. *Aids*, 29(7):819–824, 2015.
- [11] Centers for Disease Control, Prevention, et al. Preexposure prophylaxis for the prevention of HIV infection in the United States–2021 update. *Atlanta, GA: CDC*, 2021.
- [12] Food and Drug Administration. FDA Approves First Injectable Treatment for HIV Pre-Exposure Prevention, 2021.
- [13] Anthony S Fauci, Robert R Redfield, George Sigounas, Michael D Weahkee, and Brett P Giroir. Ending the HIV epidemic: a plan for the United States. *Jama*, 321(9):844–845, 2019.
- [14] Centers for Disease Control and Prevention. Core Indicators for Monitoring the Ending the HIV Epidemic Initiative (Preliminary Data): National HIV Surveillance System Data Reported through June 2023; and Preexposure Prophylaxis (PrEP) Data Reported through March 2023. *HIV Surveillance Data Tables*, 4(4), 2023.
- [15] Laurel Bates, Amanda Honeycutt, Sarah Bass, Timothy A Green, and Paul G Farnham. Updated estimates of the number of men who have sex with men (MSM) with indications for HIV pre-exposure prophylaxis. *JAIDS Journal of Acquired Immune Deficiency Syndromes*, 88(4):e28–e30, 2021.
- [16] Centers for Disease Control and Prevention. Monitoring Selected National HIV Prevention and Care Objectives By Using HIV Surveillance Data United States and 6 Dependent Areas, 2019. *HIV Surveillance Report*, 26(2), 2021.
- [17] Weiming Zhu, A Huang Ya-lin, Athena P Kourtis, Robyn Neblett-Fanfair, Jonathan Mermin, and Karen W Hoover. Trends in HIV preexposure prophylaxis use before and after launch of the Ending the HIV Epidemic in the US initiative, 2016–2023. *JAIDS Journal of Acquired Immune Deficiency Syndromes*, pages 10–1097, 2025.
- [18] Kristopher J Jackson, Sandra I McCoy, and Douglas AE White. A decade of HIV preexposure prophylaxis (PrEP): Overcoming access barriers in the United States through expanded delivery. *Public Health Reports*, page 00333549231208487, 2023.
- [19] Athena P Kourtis, Jeffrey Wiener, Weiming Zhu, Minttu M Rönn, Joshua Salomon, Ya-Lin A Huang, Cynthia Lyles, Rupa R Patel, Karen W Hoover, Robyn Neblett Fanfair, et al. Estimating the population need for preexposure prophylaxis for HIV in the United States. *Annals of Epidemiology*, 2025.
- [20] Carl Schmid, Kevin Herwig, Amanda Honeycutt, Sophia D’Angelo, Adam Vincent, and MPP Laurel Bates. US PrEP Cost Analysis. 2022.
- [21] Nidhi Khurana, Emine Yaylali, Paul G Farnham, Katherine A Hicks, Benjamin T Allaire, Evin Jacobson, and Stephanie L Sansom. Impact of improved HIV care and treatment on PrEP effectiveness in the United States, 2016–2020. *JAIDS Journal of Acquired Immune Deficiency Syndromes*, 78(4):399–405, 2018.
- [22] Alex Viguerie, Chiara Piazzola, Md Islam, and Evin Jacobson. Input-output reduced order modeling for public health intervention evaluation. In *Proceedings of the 16th World Congress on Computational Mechanics and 4th Pan American Congress on Computational Mechanics*, 2024.
- [23] Stephanie L Sansom, Katherine A Hicks, Justin Carrico, Evin U Jacobson, Ram K Shrestha, Timothy A Green, and David W Purcell. Optimal allocation of societal HIV prevention resources to reduce HIV incidence in the United States. *American Journal of Public Health*, 111(1):150–158, 2021.
- [24] Deven T Hamilton, Karen W Hoover, Dawn K Smith, Kevin P Delaney, Li Yan Wang, Jingjing Li, Tamika Hoyte, Samuel M Jenness, and Steven M Goodreau. Achieving the “ending the HIV epidemic in the US” incidence reduction goals among at-risk populations in the south. *BMC Public Health*, 23(1):716, 2023.
- [25] Andrea Pugliese. Contact matrices for multipopulation epidemic models: how to build a consistent matrix close to data. *Mathematical Medicine and Biology: A Journal of the IMA*, 8(4):249–271, 1991.
- [26] John Glasser, Zhilan Feng, Andrew Moylan, Sara Del Valle, and Carlos Castillo-Chavez. Mixing in age-structured population models of infectious diseases. *Mathematical Biosciences*, 235(1):1–7, 2012.
- [27] Andrew N Hill, John W Glasser, and Zhilan Feng. Implications for infectious disease models of heterogeneous mixing on control thresholds. *Journal of Mathematical Biology*, 86(4):53, 2023.
- [28] Zhilan Feng, Andrew N Hill, Philip J Smith, and John W Glasser. An elaboration of theory about preventing outbreaks in homogeneous populations to include heterogeneity or preferential mixing. *Journal of theoretical biology*, 386:177–187, 2015.
- [29] John A Jacquez, Carl P Simon, James Koopman, Lisa Sattenspiel, and Timothy Perry. Modeling and analyzing HIV transmission: the effect of contact patterns. *Mathematical Biosciences*, 92(2):119–199, 1988.

- [30] Elamin H Elbasha and Abba B Gumel. Vaccination and herd immunity thresholds in heterogeneous populations. Journal of mathematical biology, 83(6):73, 2021.
- [31] Binod Pant and Abba B Gumel. Mathematical assessment of the roles of age heterogeneity and vaccination on the dynamics and control of sars-cov-2. Infectious Disease Modelling, 9(3):828–874, 2024.
- [32] Kiesha Prem, Alex R Cook, and Mark Jit. Projecting social contact matrices in 152 countries using contact surveys and demographic data. PLoS computational biology, 13(9):e1005697, 2017.
- [33] Susan P Buchbinder, David V Glidden, Albert Y Liu, Vanessa McMahan, Juan V Guanira, Kenneth H Mayer, Pedro Goicochea, and Robert M Grant. Who should be offered HIV pre-exposure prophylaxis (PrEP)? A secondary analysis of a phase 3 PrEP efficacy trial in men who have sex with men and transgender women. The Lancet infectious diseases, 14(6):468, 2014.
- [34] Charles I Okwundu, Olalekan A Uthman, and Christy AN Okoromah. Antiretroviral pre-exposure prophylaxis (PrEP) for preventing HIV in high-risk individuals. Cochrane database of systematic reviews, (7), 2012.
- [35] Richard A Elion, Mina Kabiri, Kenneth H Mayer, David A Wohl, Joshua Cohen, Anne C Beaubrun, and Frederick L Altice. Estimated impact of targeted pre-exposure prophylaxis: strategies for men who have sex with men in the United States. International journal of environmental research and public health, 16(9):1592, 2019.
- [36] Yao-Hsuan Chen, Paul G Farnham, Katherine A Hicks, and Stephanie L Sansom. Estimating the HIV effective reproduction number in the United States and evaluating HIV elimination strategies. Journal of Public Health Management and Practice, 28(2):152–161, 2022.
- [37] Alex Viguerie, Evin U Jacobson, Katherine A Hicks, Laurel Bates, Justin Carrico, Amanda Honeycutt, Cindy Lyles, and Paul G Farnham. Assessing the impact of covid-19 on HIV outcomes in the united States: A modeling study. Sexually Transmitted Diseases, pages 10–1097, 2023.
- [38] Alex Viguerie, Jesse O’Shea, Marie Johnston, Daniel Schreiber, Joella Adams, Laurel Bates, Justin Carrico, Katherine A Hicks, Cynthia M Lyles, and Paul G Farnham. Impact of increased uptake of long-acting injectable antiretroviral therapy on HIV incidence and viral suppression in the United States under 2021 FDA guidelines. AIDS, pages 10–1097, 2025.
- [39] Bruno Sudret. Global sensitivity analysis using polynomial chaos expansions. Reliability engineering & system safety, 93(7):964–979, 2008.
- [40] Chiara Piazzola, Lorenzo Tamellini, and Raul Tempone. A note on tools for prediction under uncertainty and identifiability of SIR-like dynamical systems for epidemiology. Mathematical Biosciences, 332:108514, 2021.
- [41] Vangipuram Lakshmikantham and Srinivasa Leela. Differential and integral inequalities: theory and applications: volume I: ordinary differential equations. Academic press, 1969.
- [42] Herbert W Hethcote. The mathematics of infectious diseases. SIAM review, 42(4):599–653, 2000.
- [43] Pauline van den Driessche and James Watmough. Reproduction numbers and sub-threshold endemic equilibria for compartmental models of disease transmission. Mathematical Biosciences, 180(1-2):29–48, 2002.
- [44] Odo Diekmann, Johan Andre Peter Heesterbeek, and Johan Anton Jacob Metz. On the definition and the computation of the basic reproduction ratio R_0 in models for infectious diseases in heterogeneous populations. Journal of Mathematical Biology, 28:365–382, 1990.
- [45] Roy M Anderson and Robert M May. Population biology of infectious diseases: Part i. Nature, 280(5721):361–367, 1979.
- [46] United States Census Bureau. Georgia - Census Bureau Profile, 2023.
- [47] Kerith J Conron and Shoshana K Goldberg. Adult LGBT population in the United States. 2019.
- [48] Alex Viguerie, Ruiguang Song, Anna Satcher Johnson, Cynthia M Lyles, Angela Hernandez, and Paul G Farnham. COVID-related Excess Missed HIV Diagnoses in the United States in 2021: Follow-up to 2020. AIDS, pages 10–1097, 2025.
- [49] D Allen Roberts, Daniel Bridenbecker, Jessica E Haberer, Ruanne V Barnabas, and Adam Akullian. The impact of prevention-effective prep use on hiv incidence: a mathematical modelling study. Journal of the International AIDS Society, 25(11):e26034, 2022.
- [50] Ilya M Sobol. Global sensitivity indices for nonlinear mathematical models and their Monte Carlo estimates. Mathematics and computers in simulation, 55(1-3):271–280, 2001.
- [51] Norbert Wiener. The homogeneous chaos. American Journal of Mathematics, 60(4):897–936, 1938.
- [52] Dongbin Xiu and George Em Karniadakis. The Wiener–Askey polynomial chaos for stochastic differential equations. SIAM Journal on Scientific Computing, 24(2):619–644, 2002.

- [53] Oliver G. Ernst, Antje Mugler, Hans-Jörg Starkloff, and Elisabeth Ullmann. On the convergence of generalized polynomial chaos expansions. *ESAIM: M2AN*, 46(2):317–339, 2012.
- [54] Sébastien Da Veiga, Fabrice Gamboa, Bertrand Iooss, and Clémentine Prieur. *Basics and Trends in Sensitivity Analysis*. Society for Industrial and Applied Mathematics, Philadelphia, PA, 2021.
- [55] A. Saltelli, M. Ratto, T. Andres, F. Campolongo, J. Cariboni, D. Gatelli, M. Saisana, and S. Tarantola. *Global sensitivity analysis: the primer*. John Wiley & Sons, 2008.
- [56] Chiara Piazzola and Lorenzo Tamellini. Algorithm 1040: The Sparse Grids Matlab Kit - a Matlab implementation of sparse grids for high-dimensional function approximation and uncertainty quantification. *ACM Transactions on Mathematical Software*, 50(1), 2024.
- [57] C. Piazzola and L. Tamellini. The Sparse Grids Matlab Kit - v. 23-5 Robert, 2023. <https://github.com/lorenzo-tamellini/sparse-grids-matlab-kit>.
- [58] Hans-Joachim Bungartz and Michael Griebel. Sparse grids. *Acta Numerica*, 13:147–269, 2004.
- [59] Salman Safdar, Calistus N Ngonghala, and Abba B Gumel. Mathematical assessment of the role of waning and boosting immunity against the BA. 1 Omicron variant in the United States. *medRxiv*, pages 2022–07, 2022.
- [60] Salman Safdar and Abba B Gumel. Mathematical assessment of the role of interventions against SARS-CoV-2. In *Mathematics of Public Health: Mathematical Modelling from the Next Generation*, pages 243–294. Springer, 2023.
- [61] Calistus N Ngonghala, Hemaho B Taboe, Salman Safdar, and Abba B Gumel. Unraveling the dynamics of the omicron and delta variants of the 2019 coronavirus in the presence of vaccination, mask usage, and antiviral treatment. *Applied mathematical modelling*, 114:447–465, 2023.
- [62] Abba B Gumel, Connell C McCluskey, and Pauline van den Driessche. Mathematical study of a staged-progression HIV model with imperfect vaccine. *Bulletin of Mathematical Biology*, 68:2105–2128, 2006.
- [63] Queen Tollett, Salman Safdar, and Abba B Gumel. Dynamics of a two-group model for assessing the impacts of pre-exposure prophylaxis, testing and risk behaviour change on the spread and control of HIV/AIDS in an MSM population. *Infectious Disease Modelling*, 9(1):103–127, 2024.